CONFIDENTIAL

NACA RM A50H09

NACA

RESEARCH MEMORANDUM

THE USE OF AREA SUCTION FOR THE PURPOSE OF DELAYING SEPARATION OF AIR FLOW AT THE LEADING EDGE OF A 63° SWEPT-BACK WING

By Woodrow L. Cook, Roy N. Griffin, Jr., and Gerald M. McCormack

Ames Aeronautical Laboratory
Moffett Field, Calif.

NATIONAL ADVISORY COMMITTEE FOR AERONAUTICS

WASHINGTON

November 22, 1950

CONFIDENTIAL

NATIONAL ADVISORY COMMITTEE FOR AERONAUTICS

RESEARCH MEMORANDUM

THE USE OF AREA SUCTION FOR THE PURPOSE OF DELAYING SEPARATION OF AIR FLOW AT THE LEADING EDGE OF A 63° SWEPT-BACK WING

By Woodrow L. Cook, Roy N. Griffin, Jr., and
Gerald M. McCormack

SUMMARY

An investigation was conducted to determine the effectiveness of area suction used to delay the separation of air flow at the leading edge of a 63° swept-back wing. Changes in lift, drag, and pitching-moment data were correlated with the occurrence of the separation of the air flow by means of pressure-distribution data. The major portion of the investigation dealt with the delay effected in air-flow separation from the leading edge as the chordwise extent of area suction was varied, suction being applied over the full span through a surface of constant porosity. Some tests were made with the degree of porosity varied chordwise.

The effectiveness of area suction and its applicability to three-dimensional swept wings were verified by the improvements made on the static longitudinal characteristics of the wing. The largest improvements were made with the chordwise extent of area suction varied approximately linearly from about 1.2 percent of the streamwise chord at the root to 3.5 percent at the 75-percent span and then held constant at a value of 3.5 percent from 75-percent span to the tip. With this distribution of area suction separation occurred at a lift coefficient of 0.67 with a flow coefficient of 0.0029, whereas without suction separation occurred at a lift coefficient of 0.25.

Correlations between experimental results and theory were made. It was found that the spanwise and the chordwise extent of area suction required to control leading-edge separation were in general agreement with that predicted by theory, but the quantity of flow required was considerably higher than predicted by theory.

INTRODUCTION

A previous investigation (reference 1) has shown that the 63° swept-back wing under study has unsatisfactory longitudinal characteristics

(lift, drag, and pitching moment) beginning at a wing lift coefficient of about 0.2. These characteristics were believed to be the result of separation of air flow at the leading edge of the wing (hereafter called leading-edge separation). At this lift coefficient, separation started at the tip sections and, as the angle of attack was increased, rapidly progressed spanwise toward the root of the wing. The occurrence of separation and its progression caused large increases in the rate of drag rise. Also, the pitching moments indicated first a rapid movement of the aerodynamic center from the 38-percent station of the mean aerodynamic chord to the 60-percent station at a lift coefficient of 0.4. This was followed by a more rapid forward movement of the aerodynamic center to a point 12 percent ahead of the leading edge of the mean aerodynamic chord as the lift coefficient was increased to about 0.6.

The theory of reference 2 indicated that the occurrence of leading-edge separation could be eliminated by increasing the stability of the laminar boundary layer with the removal of extremely small quantities of air from the boundary layer by applying continuous suction through a porous surface. According to the theory, this type of boundary-layer control (area suction) should be applied at the leading edge where additional-type lift due to angle of attack produces severe adverse pressure gradients that are conducive to an unstable laminar boundary layer and hence to separation. Two-dimensional tests (reference 3) have at least qualitatively verified the theory.

The applicability of the theory to the three-dimensional case had not been studied experimentally. Many questions existed and, in particular, the question regarding the influence of the spanwise flow of the boundary-layer air, characteristic of swept wings, on the effectiveness of area suction. Therefore, to examine, in general, the effectiveness of such boundary-layer control applied to swept wings and, in particular, to determine the improvements that could be made on the longitudinal characteristics of the 63° swept-back wing, an investigation was conducted in the Ames 40- by 80-foot wind tunnel. The results of the investigation are presented in this report.

NOTATION

The data are presented in the form of standard NACA coefficients and symbols which are defined as follows:

a.c. aerodynamic center measured in percent chord aft of the leading edge of the mean aerodynamic chord

b wing span, feet

c chord, measured parallel to the plane of symmetry, feet

$\bar{c}$ mean aerodynamic chord $\left(\frac{\int_0^{b/2} c^2\,dy}{\int_0^{b/2} c\,dy}\right)$, feet

c_l section lift coefficient $\left(\frac{1}{c}\int_0^c P\,dx\cos\alpha - \frac{1}{c}\int_0^t P\,dz\sin\alpha\right)$

c_n section normal-force coefficient $\left(\frac{1}{c}\int_0^c P\,dx\right)$

c_{w_o} porosity factor for the porous material $\left(\frac{w_o \mu t}{\Delta p}\right)$, square feet

C_D drag coefficient $\left(\frac{\text{drag}}{qS}\right)$

C_L lift coefficient $\left(\frac{\text{lift}}{qS}\right)$

C_m pitching-moment coefficient computed about the quarter-chord point of the mean aerodynamic chord $\left(\frac{\text{pitching moment}}{qS\bar{c}}\right)$

C_Q flow coefficient $\left(\frac{Q}{U_o S}\right)$

H shape parameter $\left(\frac{\delta^*}{\theta}\right)$

p free-stream static pressure, pounds per square foot

p_l local static pressure, pounds per square foot

P airfoil pressure coefficient $\left(\frac{p_l - p}{q}\right)$

q free-stream dynamic pressure, pounds per square foot

Q volume of air removed through porous surface, cubic feet per second based on standard density

R Reynolds number $\left(\frac{U_o \bar{c}}{\nu}\right)$

S wing area, square feet

t airfoil thickness, feet, or thickness of the porous material, feet

u local velocity parallel to surface and inside boundary layer, feet per second

U local velocity parallel to surface at outer edge of boundary layer, feet per second

U_{max} maximum local velocity, feet per second

w_o suction-air velocity normal to surface, feet per second

$w_o(x)$ velocity normal to the surface as a function of x, feet per second

U_o free-stream air velocity, feet per second

x chordwise coordinate parallel to plane of symmetry, feet

y spanwise coordinate perpendicular to plane of symmetry, feet

z ordinate to airfoil surface normal to chord line and boundary-layer coordinate normal to the surface, feet

α angle of attack of chord plane of basic wing, degrees

δ^* displacement thickness $\left[\int_o^\infty \left(1 - \frac{u}{U} \right) dz \right]$, feet

Δp pressure drop across porous material, pounds per square foot

θ momentum thickness $\left[\int_o^\infty \frac{u}{U} \left(1 - \frac{u}{U} \right) dz \right]$, feet

μ coefficient of viscosity, slugs per foot-second

ν kinematic coefficient of viscosity, square feet per second

MODEL AND APPARATUS

The geometric characteristics of the model are shown in figures 1, 2, and 3. The wing had 63° sweepback of the leading edge, an aspect ratio of 3.5, and a taper ratio of 0.25. There was 0° twist, dihedral, and incidence. The wing sections were constant across the span and were NACA 64A006 sections parallel to the plane of symmetry.

The fuselage had a fineness ratio of 10.5 based on actual fuselage length. The cross section of the fuselage was circular except where the air-exhaust duct projected beneath the lower surface. A photograph of the model as mounted for testing in the wind tunnel is shown in figure 4.

The leading-edge portion of the wing was constructed of a continuous metal-mesh sheet extending from 5 percent of the streamwise chord on the lower surface of the wing to 20 percent of the streamwise chord on the upper surface. The mesh sheet was 0.01 inch thick, had 1600 holes per square inch, and had 19-percent open area. Aircraft linen tape and linen tape which had been sprayed with varying numbers of coats of aircraft dope were used to cover that portion of the leading edge where suction was to be applied. The portion of the leading edge where suction was not to be applied was covered with a nonporous cellulose tape of 0.0032-inch thickness.

Calibration tests were made of the flow resistance of the porous materials used on the leading edge of the wing. These tests were made with no flow tangential to the surface. The calibration curves for the porous materials used are shown in figure 5. From the figure, it can be seen that, for the plain linen surface, a pressure differential of 45 pounds per square foot[1] was required to induce a velocity of 4 feet per second through the surface, and for the linen surface sprayed with 5 coats of dope a pressure differential of 145 pounds per square foot was required to induce the same velocity.[2]

The pump for creating suction was installed inside the fuselage. It was a high-speed centrifugal compressor driven by a variable-speed electric motor.

The air was induced through the porous leading edges of the wings, continued through the spanwise ducts, and was dumped into the fuselage, which was sealed to the outside and served as a plenum chamber in the system. The air was then drawn through the pump and was ejected through the exhaust duct beneath the fuselage.

To measure the quantity of air flowing through the system, survey rakes were used. The rakes were composed of 54 total-pressure tubes and 6 static-pressure tubes and were located 3/4 inch inside the exit of the exhaust duct.

Internal pressures within the leading-edge duct were measured with static-pressure orifices. Since the velocities of the air inside the duct

---

[1]This corresponds to a porosity factor of $c_{w_o} = 0.504 \times 10^{-10}$ feet squared, assuming constant porosity through the 0.018-inch thickness at standard atmospheric conditions.

[2]This corresponds to a porosity factor of $c_{w_o} = 0.1564 \times 10^{-10}$ feet squared.

were very low, the indicated static pressures were assumed to be substantially equal to the total pressure.

Static pressure orifices were positioned over the upper and lower surfaces of streamwise sections located at five stations from 30.0- to 90.0-percent semispan. The spanwise and chordwise positions of the orifices are listed in table I.

TESTS

Force and pressure-distribution measurements were made through an angle-of-attack range at zero sideslip. The data were obtained at a velocity of approximately 63 miles per hour (Reynolds number of 4.9×10^6 based on a mean aerodynamic chord of 8.64 feet). The tests were made at low velocities in order to obtain a higher flow coefficient for boundary-layer control.

The majority of the tests were conducted with area suction applied to the entire span of the leading edge of the wing with porosity of the surface kept constant and with the chordwise extent of suction being the variable. Limited tests were made of the effect of varying the porosity of the surface chordwise with full-span area suction and of the effect of varying the spanwise extent of area suction with the porosity and the chordwise extent of area suction held constant. Of the configurations tested, those to be discussed herein are listed in the table, figure 2.

CORRECTIONS

Standard tunnel-wall corrections for a straight wing of the same area and span as the swept-back wing have been applied to angle-of-attack and drag-coefficient data. This procedure was followed since a brief approximate analysis indicated that tunnel-wall corrections were approximately the same for straight and swept wings of the size under consideration. The corrections applied are as follows:

$$\Delta\alpha = 0.48\ C_L$$

$$\Delta C_D = .0084\ C_L^2$$

No corrections have been applied for the drag and interference of the struts since they were unknown. Pitching-moment tares were not applied since they were not of sufficient magnitude to significantly affect the results. All flow coefficients were corrected to standard sea-level temperature conditions. No corrections were made for the jet effect of the exhause air since calculations indicated that the corrections would be very small.

RESULTS AND DISCUSSION

Basic Wing

The lift, drag, and pitching-moment characteristics of the 63° swept-back wing of this test are shown in figure 6 and are very similar to the results discussed in reference 1. Up to a lift coefficient of about 0.25, the drag increased at the normal rate (as induced drag) and the lift curve and the pitching-moment curve were approximately linear. From this lift coefficient to the maximum lift coefficient of about 1.27, the drag increased at a high rate and the lift-curve slope first increased and then decreased as maximum lift was approached. Between lift coefficients of about 0.25 to 0.4, the pitching-moment curve indicated that the aerodynamic center moved aft from the 38-percent point of the mean aerodynamic chord to the 60-percent point. As the lift coefficient was increased above 0.4, the aerodynamic center moved very rapidly forward to a position 10 percent ahead of the leading edge of the mean aerodynamic chord.

A study of the pressure distributions (fig. 7) showed the cause of the poor longitudinal characteristics just described. The pressure distribution followed a similar pattern at the various spanwise stations. As the angle of attack was increased above a certain angle at each station, the rate of rise of the pressure peak at the leading edge decreased (e.g., by 6.2° angle of attack, the rate of rise of the peak pressure had already decreased at the 90-percent station), resulting in a slight decrease in section lift-curve slope as shown in figure 8. At a slightly higher angle of attack, a maximum peak pressure was reached. Further increases in angle of attack resulted in a decrease in the magnitude of the peak pressure and a chordwise redistribution of the section load (e.g., by 7.2° angle of attack, the maximum peak pressure had been reached and exceeded at the 90-percent station although it had not yet fallen to that existing at 6.2° angle of attack), resulting in an increase in section lift-curve slope and a rearward movement of the center of pressure. These changes are believed to result from separation of the air flow from the wing leading edge. Comparison of pressure distributions obtained in this investigation with those of reference 4 obtained from two-dimensional tests of the same section shows marked similarity. Following the analysis of reference 4 it can be presumed that here also the separation was occurring in the laminary boundary layer and, at the angle of attack where separation first appeared, was followed by reattachment of the air flow. As the angle of attack was further increased, the point of reattachment progressed chordwise until separation occurred over the entire chord (e.g., at 90-percent span $\alpha \cong 9.2°$). This chordwise progression of separation was similar at each station but occurred at progressively higher angles of attack for the stations farther inboard.

The effect of separation on the section characteristics at various spanwise stations can be correlated with the consequent changes in the

longitudinal characteristics. Since both the previously mentioned increase in section lift-curve slope and the previously noted chordwise redistribution of section load occurred first at the outboard sections, there resulted a large rearward movement of the aerodynamic center as the angle of attack was increased from 5° to 8°. As separation moved farther inboard, the lift of the outboard sections decreased, resulting in the rapid forward movement of the aerodynamic center. The pressure distributions show that the spanwise progression of separation from tip to root was relatively rapid, being completed within an angle-of-attack increment of 6° or 7°.

From the foregoing, it is evident that the large movements of the aerodynamic center and the large increases in drag were the result of leading-edge separation. Therefore, significant improvement would result if the occurrence of separation were delayed by the application of area suction at the leading edge of the wing.

Principle of the Application of Area Suction

In view of the reasoning of the previous section, a study was made of the theory of area suction for the two-dimensional case and a method was developed to enable application of this type of boundary-layer control to the 63° swept-back wing. The basic theory of area suction has been developed by Thwaites and the procedure for its application to the two-dimensional case is demonstrated in reference 2. The theory gives, for a desired lift coefficient to be obtained without separation, the required chordwise extent of area suction and the required velocity of the suction air normal to the surface. It was assumed in the theory that the suction-air velocities were equal at all chordwise points. The velocity so determined is that required to maintain a Blasius boundary-layer profile through any given adverse velocity gradient. It is then reasoned that it is necessary to have suction extend chordwise on an airfoil section only to that point where the adverse velocity gradient corresponding to the desired lift coefficient is no more severe than the maximum velocity gradient reached without area suction just prior to separation.

Applying the theory to the data of reference 3 substantiates this reasoning. In reference 3 it was found that the most effective chordwise extent of area suction for the maximum section lift coefficient was 4.5 percent of the chord. This is the same chordwise extent that would be estimated by the method used in conjunction with the foregoing reasoning.

Before the section theory can be applied to a three-dimensional wing, a method must be developed to determine the required spanwise extent of area suction. In doing this, it is necessary to determine the section lift at which separation first occurs at each spanwise station and then to find the section lift coefficients for each station corresponding to any

desired wing lift coefficient. Thus, the necessary increment of section lift is established and, with the assumption that each station can be treated independently, the chordwise extent of area suction at any spanwise point required can be determined.

For the 63° swept-back wing, the spanwise progression of separation was obtained from the pressure distributions of the basic wing. This progression of separation is shown in figure 9 by the dashed line passing through the section lift coefficient at each section just prior to separation at that section. Theoretical spanwise variations of section lift for the wing (obtained from reference 5) are shown in the figure for four values of wing lift coefficient in order to demonstrate the spanwise extent of suction necessary for each lift coefficient. For a wing lift coefficient of 0.25, the dashed line does not cross the span loading line; hence no suction is needed. For a wing lift coefficient of 0.4, the dashed line crosses the span loading line at 50-percent span; hence suction is necessary over the outboard 50-percent span of the wing. For wing lift coefficients of 0.5 and 0.62, the dashed line does not cross the span-loading curves outboard of the fuselage; hence suction is necessary over the full span of the wing.

After determining the spanwise extent of area suction required to reach a given lift coefficient without separation, it is necessary to find the chordwise extent of area suction required at each of the various stations. This is accomplished by calculating for each station the pressure or velocity distribution that would exist just prior to separation at the section without suction, and also that which would correspond to the desired wing lift coefficient with separation prevented by suction. With the velocity distributions known, the method of reference 2 can be applied to find the chordwise extent of area suction required at each station.

To illustrate the foregoing procedure quantitatively, a sample of the method used for the 63° swept-back wing is included. The station for which the required chordwise extent of area suction is to be determined is the 75-percent-span point, and the lift coefficient to be attained without separation is 0.62. Shown in figure 10 are (a) the velocity distribution,[3]

[3]The velocity distributions are calculated normal to the leading edge in this report. An unpublished analysis shows that the theoretical pressure distributions calculated by the method given in NACA Rep. 833 (reference 6) can be adjusted for the effects of sweep by use of the following equation for the upper surface pressures for a symmetrical section:

$$P_u = \left[1 - \left(\frac{U}{U_o} + c_l K \frac{P_a}{4(U/U_o)}\right)^2\right] \cos^2 \Lambda_l$$

where P_u is the upper surface pressure and P_a is the pressure due to additional lift,

$$K = \frac{1}{\int_0^1 P_a \cos^2 \Lambda_l \, d(x/c)}$$

Λ_l is the sweep angle for locus of constant percent chord points and U/U_o is the local velocity ratio due to basic airfoil thickness.

just prior to separation at the section (c_l = 0.45, C_L = 0.34); and (b) the velocity distribution for the desired section lift coefficient at the section (c_l = 0.81, C_L = 0.62). Since it is difficult to determine the exact point of the chordwise extent of area suction by the reasoning of Thwaites from a comparison of very steep adverse pressure gradients, the following conservative and simplifying approximation was made. A horizontal line was drawn from the maximum velocity point of curve (a) to intersect curve (b) and thus define the chordwise extent of suction. It is evident that the extent of area will be slightly greater than that predicted by Thwaites. In this case, the chordwise extent of suction was found to be 2.7 percent of the chord. This procedure has been applied to the other wing stations and for other wing lift coefficients. The results are given in figure 11 and show that, as the section is nearer the tip, the required chordwise extent of suction is greater for any given lift coefficient.

The theory can then be used to determine the suction-air velocities at various spanwise stations required to maintain unseparated flow to a given lift coefficient. With the spanwise and chordwise extents determined, the total-flow coefficient required can then be found. In reference 2 (see also the appendix herein) a relation is developed between a velocity gradient and the suction-air velocity required to maintain a Blasius boundary-layer profile in that velocity gradient. The equation expressing this relation is as follows:

$$\frac{x w_o^2}{\nu U_{max}} = 4.53453 \left(\frac{U}{U_{max}} \log \frac{U}{U_{max}} - \frac{U}{U_{max}} + 1 \right)$$

where

w_o suction-air velocity measured normal to the wing surface

U local velocity parallel to the wing surface

U_{max} maximum local velocity

A plot is made in the form of U/U_{max} as a function of x/c of the section velocity distribution at the desired lift coefficient. In this same figure U/U_{max} is plotted as a function of the new parameter $\frac{x w_o^2}{\nu U_{max}}$ by means of the previously given relation. The abscissa scale is chosen so that the resulting curve is at least as steep at all points as the curve of the section velocity distribution. The suction velocity can be determined by the use of the relation between the abscissa scales in the following manner:

$$\frac{x w_o^2}{\nu U_{max}} \div \frac{x}{c} = \frac{c w_o^2}{\nu U_{max}}$$

For a given section lift coefficient

$$\frac{cw_o^2}{\nu U_{max}} = K$$

where K is a numerical value (the absolute value of ratio of the of the abscissa scales), from which

$$w_o^2 = K \frac{\nu}{c} U_{max} \left(\frac{U_o^2}{U_o^2}\right)$$

where U_o is the free-stream velocity normal to the leading edge and then

$$w_o = U_o \sqrt{K \left(\frac{U}{U_o}\right)_{max} \frac{1}{R}}$$

where R is the section Reynolds number. As previously noted, the theory assumes that this suction-air velocity is constant for all chordwise points. Hence, when this velocity has been determined for each spanwise station, the total flow quantity can also be determined.

An example of the application of the foregoing procedure is given in figure 12. These results are for the same station (75-percent span) and the same wing lift coefficient (C_L = 0.62) as used in the example illustrating the determination of the chordwise extent of suction. Applying the procedure to all spanwise stations gave a flow coefficient of 0.00005 for the wing of this investigation for a wing lift coefficient of 0.62.

A comparison of the flow coefficients found necessary experimentally in the subject investigation with those predicted by the foregoing process could not be expected to show good agreement. It must be pointed out that in a majority of the tests the model was constructed with a surface of constant porosity. Hence, with constant internal pressures, the suction-air velocity would vary chordwise since the external pressure varies chordwise. To take this variation into account, it can be assumed that the suction-air velocity found by the theory would be the velocity required at the leading edge at each station and, rearward of this point, the suction-air velocity would increase as the negative section pressures decrease. Such a calculation showed that the condition of constant porosity chordwise increased the flow coefficient required for a wing lift coefficient

of 0.62 to 0.0005, or 10 times that for the case of constant suction-air velocities at all chordwise points. A comparison of the flow coefficients for the two conditions of chordwise variation of suction-air velocity is shown as a function of lift coefficient in figure 13.

In summary, therefore, the application of the theory to the 63° swept-back wing indicates that, to obtain a lift coefficient of 0.62 without separation, full-span area suction is required; the chordwise extent of the suction varies from about 3.2 percent at the tip to about 0.8 percent at the root. The flow coefficient required is indicated to be 0.00005 if constant velocities are obtained, and 0.0005 if the porosity of the surface is equal at all points on the chord of a particular section.

Experimental Results of Area Suction

The experimental investigation was undertaken with two end points in view: first, to determine if the concept of area suction was valid in the case of the swept wing, and second, to relate qualitatively the results to those anticipated from theoretical considerations. The first point is relatively simple to determine since any significant delay in the occurrence of separation would serve as proof. The second is considerably more difficult for several reasons. The theory requires that, for a desired value of lift coefficient, precise distribution of suction area and suction velocities be obtained. A test model thus designed for one value of lift coefficient would be too inflexible in construction to make a general study of the applicability of area suction. Further, it was considered likely that three-dimensional effects would cause the results to deviate from theory and a study of conditions other than those of the design point would be required. The preliminary studies were therefore made with only an approximation of the required distribution of suction area and with little or no attempt to control the spanwise or chordwise distribution of suction velocity. Only qualitative agreement with theory can therefore be expected.

Full-span area suction.- The theory indicated that, to make appreciable gains in the lift coefficient without separation, it would be necessary to apply suction to the full span of the wing; thus a majority of the tests were made with full-span area suction. The effects of three variations of chordwise extent of area suction were investigated; these distributions corresponded approximately to those required by theory to give lift coefficients of 0.45, 0.55, and 0.65. The three distributions are tabulated in the following table:

Model configuration	Percent local streamwise chord				
	0.30 b/2	0.45 b/2	0.60 b/2	0.75 b/2	0.90 b/2
A, C_L = 0.65	1.5	1.9	2.5	3.5	3.5
D, C_L = .55	1.0	1.5	2.5	2.5	2.5
E, C_L = .45	.5	.7	1.0	1.5	1.5

The lift, drag, and pitching-moment characteristics for each configuration with the flow coefficient near the maximum obtainable are shown in figure 14(a). It can be seen that for the respective configurations the lift coefficient of 0.45 was exceeded; whereas the lift coefficient of 0.55 was just obtained, and the lift coefficient of 0.65 was not reached with the available flow coefficient before separation occurred.

The effect of reduced flow coefficients (fig. 14(b)) in two cases showed that the lift coefficient of 0.55 was still obtained on configuration D, but a sharp drop in lift coefficient occurred with decreased flow coefficient in the case of configuration A. It was evident, therefore, that the maximum useful flow coefficient was reached in the first case but not in the second, and further gains should result if the flow coefficient could be increased for configuration A.

The construction of the pump was altered to allow higher flow coefficients to be obtained. With the increased flow, additional tests were made of configuration A. Figures 15(a) and (b) show the longitudinal characteristics of the model for various flow coefficients. It can be seen that, at the maximum flow coefficient, the design lift coefficient was reached and it appears that greater flow quantities would produce further gains in lift coefficient. It is also evident that relatively small decreases in flow quantity result in significant reductions of the gains due to the application of suction in the case where the flow coefficient is marginal as was the case in the tests.

It is of interest to compare the total flow coefficient estimated by theory to that actually used even though no attempt was made to control the flow distribution in this case. From figure 13, a value of 0.00065 (assuming constant porosity) is shown to be required to reach a lift coefficient of 0.67; whereas 0.0029 was required in the experimental investigation. However, it must be pointed out that the chordwise extent of area suction was greater at all points along the span in the actual investigation than the estimated values taken from figure 11. Also it was clear from the examination of the duct pressures that excess air was removed from all the sections inboard of 75-percent span. Therefore, it seems safe to assume that, if the model had more accurately met the conditions of theory, the experimental flow quantity would be closer to that given by theory.

The application of area suction markedly affected the section characteristics as can be seen by a comparison of the section pressure distributions with suction applied (fig. 16) to those with no suction applied (fig. 7). The data of figure 16 were obtained with the suction-area distribution of configuration A and a flow coefficient of 0.0029. The maximum peak negative pressures reached with suction applied were approximately four times as great as the maximum peak pressures reached on the basic wing. The first occurrence of separation was still of the leading-edge type, but the progression of separation chordwise was altered considerably. The pressure distributions show no large chordwise redistribution of the section load prior to an angle of attack of 20.4°; the section lift curves (fig. 17) remain linear to higher section lift coefficients than on the basic wing (fig. 8). For example, at the 75-percent-spanwise station where satisfactory suction-air velocities were maintained, the section lift (based on free-stream velocity) was increased from about 0.4 to about 0.9 before separation occurred, as indicated by nonlinearity of the section lift-curve slope. The maximum section lift coefficient attained was limited by leading-edge separation; whereas two-dimensional data of thin airfoil sections with boundary-layer control applied by either porous suction (reference 3) or through the use of a slot near the leading edge (reference 7) showed the maximum lift to be limited by trailing-edge separation. It might be expected, therefore, that further gains can be made on the wing of the subject investigation.

Separation spread spanwise from the tip of the wing to the root in about the same increment of angle of attack on the wing with suction as on the basic wing. Due to the changes in the section characteristics, however, there was no rearward movement of the wing aerodynamic center.

Partial-span area suction.- In view of the possibility of strong three-dimensional effects on the wing, not taken into account by theory, some tests were made with suction applied to only the outboard portions of the wing. The spanwise extent of area suction was varied from the outboard 7-1/2 percent (the minimum extent) to the outboard 80 percent of the wing (the maximum partial-span extent).

In general, the maximum delays in separation were small and of the same order as predicted by theory. For instance, theory indicates that with suction applied only over the outboard 40 percent of the span unseparated flow would be maintained to a lift coefficient slightly less than 0.4. It can be seen in figure 18[4] that with suction applied to the outboard 40 percent of the span (configuration C, fig. 2) evidence of separation appeared between lift coefficients of 0.35 and 0.4.

[4] In figure 18 there is some variation of basic-wing data compared with that of figure 6. This is due to an external reinforcing covering that was placed over the porous surface at the inboard sections of the wing for the tests at the particular time.

For purposes of comparison, the data obtained with full-span application of suction are included in figure 18. In each case the chordwise extent of area suction over the outboard 40 percent of the span is the same. The total flow coefficients are not the same, but if the total area of suction is taken into account in each case, the average suction-air velocities at the surface would be greater for the case with suction applied only over the outboard 40 percent of the span.

From the visual observations of the pressure distributions for all the spanwise extents of area suction tested, it was apparent that the outboard sections where suction was applied did reach higher angles of attack without separation. The inboard sections, however, where suction was not applied, showed evidence of separation at the same angle of attack as for the basic wing. This can be seen in figure 19 by comparing the pressure distribution of a section at 30-percent span when partial-span suction was applied with the pressure distribution when full-span suction was applied. For an angle of attack of 11.4° separation had occurred when partial-span suction was applied, but had not occurred when full-span suction was applied.

The investigation reported in reference 8 disclosed that removing air at the root of a swept-forward wing had a strong three-dimensional effect on the occurrence of separation on the entire wing. If such a phenomenon were to exist on a swept-back wing, presumably it would occur with suction confined to the tip. Such was not found to be the case, however, in the present investigation. This may be due to the fact that a quantity of air was removed at a rate of less than 3 pounds per second; whereas in the case of the swept-forward wing about 30 pounds of air per second was removed.

Variation of the porosity of the surface.- In the development of the theory, the suction-air velocities were assumed to be equal at all chordwise points. Since the efficiency of the system would be higher with the lower total-flow coefficient obtainable in this manner, several attempts were made to vary chordwise the porosity of the surface in order to attain more uniform suction-air velocities. The surface was doped with aircraft dope in a stepwise manner with the number of coats of dope increasing from two to five from the leading edge to the rearmost point of the chordwise extent of the suction area. The purpose of this was to approximate the gradual change in porosity that would give equal suction-air velocities at all points on the chord. Figure 20 shows data obtained from test of one of the configurations (configuration F, fig. 2). Also shown in this figure are data obtained from tests of the configuration with the same distribution of suction area, but having no variation of porosity. It can be seen that the same lift coefficient was obtained prior to separation in each case but at a lower flow coefficient ($C_Q = 0.0021$ compared to $C_Q = 0.0023$) for the condition of varying porosity. It must be noted, however, that the attempts made thus far have been preliminary and are not conclusive. Further research should be undertaken to investigate

fully the possibility of realizing major reductions in flow coefficient with proper variation of the porosity of the surface.

CONCLUSIONS

The following conclusions were drawn from the results of the wind-tunnel investigation of area suction applied in the region of the leading edge of a 63° swept-back wing to delay separation of the air flow:

1. The effectiveness of area suction and its applicability to three-dimensional swept wings were verified by the delay in the occurrence of leading-edge separation. Force test data showed that significant improvements in the drag and pitching-moment characteristics of the wing resulted from the delay of leading-edge separation.

2. The largest improvements on the longitudinal characteristics were made with the chordwise extent of area suction varied approximately linearly from about 1.2 percent of the streamwise chord at the root to 3.5 percent at the 75-percent spanwise station and then held constant at a value of 3.5-percent from 75-percent span to the tip. With this distribution of area suction and a flow coefficient of 0.0029 the effects of separation were delayed from a lift coefficient of 0.25 on the basic wing to a lift coefficient of 0.67 with suction.

3. The spanwise and chordwise extent of suction area required to delay the occurrence of separation to a given lift were in general agreement with that predicted by theory. The total quantity of flow required in the investigation was considerably higher than that predicted by theory. It is believed that inadequate control of the distribution of suction-air velocities is responsible in large measure for this disagreement.

Ames Aeronautical Laboratory,
National Advisory Committee for Aeronautics,
Moffett Field, Calif.

APPENDIX

THWAITES' THEORY OF AREA SUCTION

The theory of area suction developed by Thwaites in reference 2 is included in this appendix for convenient reference. In reference 9, Thwaites derived the momentum equation of the boundary layer for a flat plate with a velocity $v_o(x)$ normal to its surface. By use of the Navier-Stokes equation for viscous fluids in steady two-dimensional flow in the form of

$$u \frac{\partial u}{\partial x} + v \frac{\partial u}{\partial y} = U \frac{dU}{dx} + \nu \frac{\partial^2 u}{\partial y^2} \tag{1}$$

and the equation of continuity

$$\frac{\partial u}{\partial x} + \frac{\partial v}{\partial y} = 0 \tag{2}$$

the momentum equation of the boundary layer can be derived (see reference 9) thus,

$$UU' (\delta^* + 2\theta) + U^2 \frac{d\theta}{dx} = w_o (x) U + \nu \left(\frac{\partial u}{\partial y} \right)_{y=0} \tag{3}$$

where U' is the total derivative of U with respect to x. This equation is also derived in reference 10.

The velocity normal to the surface $w_o(x)$ is assumed to be equal to w_o and to be constant chordwise. At the limit $y = 0$ equation (1) becomes

$$w_o \left(\frac{\partial u}{\partial y} \right)_{y=0} = UU' + \nu \left(\frac{\partial^2 u}{\partial y^2} \right)_{y=0} \tag{4}$$

Boundary-layer velocity profiles tend to the form of a Blasius profile at the leading edge of a plate in a uniform stream. Consequently, the analysis of reference 9 introduces the Blasius equations in the following form

$$\left(\frac{\partial u}{\partial y} \right)_{y=0} = 0.22053 \frac{U}{\theta} \tag{5}$$

$$\left(\frac{\partial^2 u}{\partial y^2} \right)_{y=0} = 0 \tag{6}$$

Substitution of equations (5) and (6) in equation (4) gives

$$w_o \left(0.22053 \frac{U}{\theta} \right) = UU'$$

from which

$$U' = 0.22053 \frac{w_o}{\theta} \tag{7}$$

Substitution of equation (7) in equation (5) gives

$$\left(\frac{\partial u}{\partial y}\right)_{y=0} = \frac{U'U}{w_o} \tag{8}$$

Substitution of equation (8) in equation (3) gives

$$U'U(H+2)\ \theta + U^2 \frac{d}{dx}\left(\frac{0.22053\ w_o}{U'}\right) = w_o\ U + \nu\left(\frac{UU'}{w_o}\right)$$

from which

$$0.22053\ w_o\ U \frac{d}{dx}\left(\frac{1}{U'}\right) = w_o\ [1 - (H+2)\ 0.22053\ ] + \frac{\nu}{w_o} U'$$

or

$$-0.22053\ w_o\ U \frac{U''}{(U')^2} = w_o\ [1 - (H+2)\ 0.22053] + \frac{\nu}{w_o} U' \tag{9}$$

Equation (9) is the momentum equation of the boundary layer having a Blasius velocity profile. For a Blasius profile, H has the value of 2.5911, but in order to continue the analysis the value of H is taken equal to 2.53453 to make the term $[1 - (H+2)\ 0.22053]$ equal to zero. Since the difference between the two values of H is small, then the momentum equation can be represented by the following equation with but small error

$$\frac{U''}{(U')^2} + 4.53453 \frac{\nu U'}{w_o^2 U} = 0, \quad H = 2.53453 \tag{10}$$

Equation (10) can be integrated to obtain the following:

$$-\frac{1}{U'} + 4.53453 \frac{\nu}{w_o^2} \log U + C_1 = 0 \tag{11}$$

The value of C_1 in equation (11) is determined by setting the limit $\theta = 0$ in equation (7) from which $U' = \infty$ and $U = U_{max}$ where U_{max} is the maximum local velocity. Thus

$$C_1 = -4.53453 \frac{\nu}{w_o^2} \log\ U_{max}$$

Substituting this value in equation (11) gives

$$-\frac{1}{U'}+4.53453\frac{\nu}{w_o^2}\left(\log U-\log U_{max}\right)=0 \tag{12}$$

from which

$$-1+4.53453\frac{\nu U'}{w_o^2}\log\frac{U}{U_{max}}=0 \tag{13}$$

Equation (13) can be integrated to obtain the following:

$$-x+4.53453\frac{\nu}{w_o^2}\left(U\log U-U-U\log U_{max}+C_2\right)=0 \tag{14}$$

The value of C_2 is determined from the condition that at $x=0$ $U=U_{max}$ hence $C_2=U_{max}$ Equation (14) then becomes

$$-\frac{x}{U_{max}}+4.53453\frac{\nu}{w_o^2}\left(\frac{U}{U_{max}}\log\frac{U}{U_{max}}-\frac{U}{U_{max}}+1\right)=0$$

or

$$\frac{xw_o^2}{\nu U_{max}}=4.53453\left(\frac{U}{U_{max}}\log\frac{U}{U_{max}}-\frac{U}{U_{max}}+1\right) \tag{15}$$

This equation expresses the relation between a velocity gradient U/U_{max} as a function of (x) and the suction-air velocity required to maintain a Blasius boundary-layer profile in that velocity gradient. Values of the parameter $xw_o^2/\nu U_{max}$ for values of U/U_{max} are given in the following table:

U/U_{max}	$xw_o^2/\nu U_{max}$
1.0	0
.9	.0234
.8	.0974
.7	.2282
.6	.4240
.5	.6957
.4	1.0587
.35	1.2813
.3	1.5363
.25	1.8294
.2	2.1680
.15	2.5639

The velocity distribution outside the boundary layer U in this case (fig. 21) is similar to that near the leading edge of an airfoil at high lift coefficients. Due to this similarity, the profile for this special type of flow can be used to estimate the flow quantities necessary to maintain unseparated flow on an airfoil section at high lift coefficients.

REFERENCES

1. McCormack, Gerald M., and Walling, Walter C.: Aerodynamic Study of a Wing-Fuselage Combination Employing a Wing Swept Back 63°.- Investigation of a Large-Scale Model at Low Speed. NACA RM A8D02, 1949.

2. Thwaites, B.: A Theoretical Discussion of High-Lift Aerofoils with Leading-Edge Porous Suction. R.& M.No. 2242 (8909), British A.R.C. Tech. Rep.,1946.

3. Nuber, Robert J., and Needham, James R., Jr.: Exploratory Wind-Tunnel Investigation of the Effectiveness of Area Suction in Eliminating Leading-Edge Separation Over an NACA 64_1A212 Airfoil. NACA TN 1741, 1948.

4. McCullough, George B., and Gault, Donald E.: Boundary-Layer and Stalling Characteristics of the NACA 64A006 Section. NACA TN 1923, 1949.

5. DeYoung, John D.: Theoretical Additional Span Loading Characteristics of Wings With Arbitrary Sweep, Aspect Ratio, and Taper Ratio. NACA TN 1491, 1947.

6. Allen, H. Julian: General Theory of Airfoil Sections Having Arbitrary Shape or Pressure Distribution. NACA Rep. 833, 1945.

7. McCullough, George B., and Gault, Donald E.: An Experimental Investigation of an NACA 63_1-012 Airfoil Section With Leading-Edge Suction Slots. NACA TN 1683, 1948.

8. McCormack, Gerald M., and Cook, Woodrow L.: Effects of Boundary-Layer Control on the Longitudinal Characteristics of a 45° Swept-Forward Wing-Fuselage Combination. NACA RM A9K02a, 1950.

9. Thwaites, B.: On the Flow Past a Flat Plate With Uniform Suction. British A.R.C. 9391, F.M. 887, Perf. 113, Feb. 11, 1946.

10. Schlichting, H.: Lecture Series "Boundary-Layer Theory" Part I - Laminar Flows. NACA TM 1217, 1949.

TABLE I

LOCATION OF PRESSURE ORIFICES

Spanwise positions[1] of orifices	
Station number	Percent semispan
1	30
2	45
3	60
4	75
5	90

Chordwise positions[2] of orifices (on upper and lower surfaces at each station)[3]	
Orifice number	Percent chord[4]
1	0
2	.25
3	.50
4	1.0
5	1.5
6	2.5
7	3.5
8	5.0
9	7.5
10	10.0
11	15.0
12	20.0
13	30.0
14	40.0
15	50.0
16	60.0
17	70.0
18	80.0
19	90.0
20	95.0
21	97.5

[1]Spanwise positions are measured perpendicular to the plane of symmetry.
[2]Chordwise positions are measured in percent of the streamwise chord.
[3]On all stations, orifice 8 on the lower surface was omitted.
[4]On station 3, upper-surface orifice 10 was located at 12.5-percent chord.

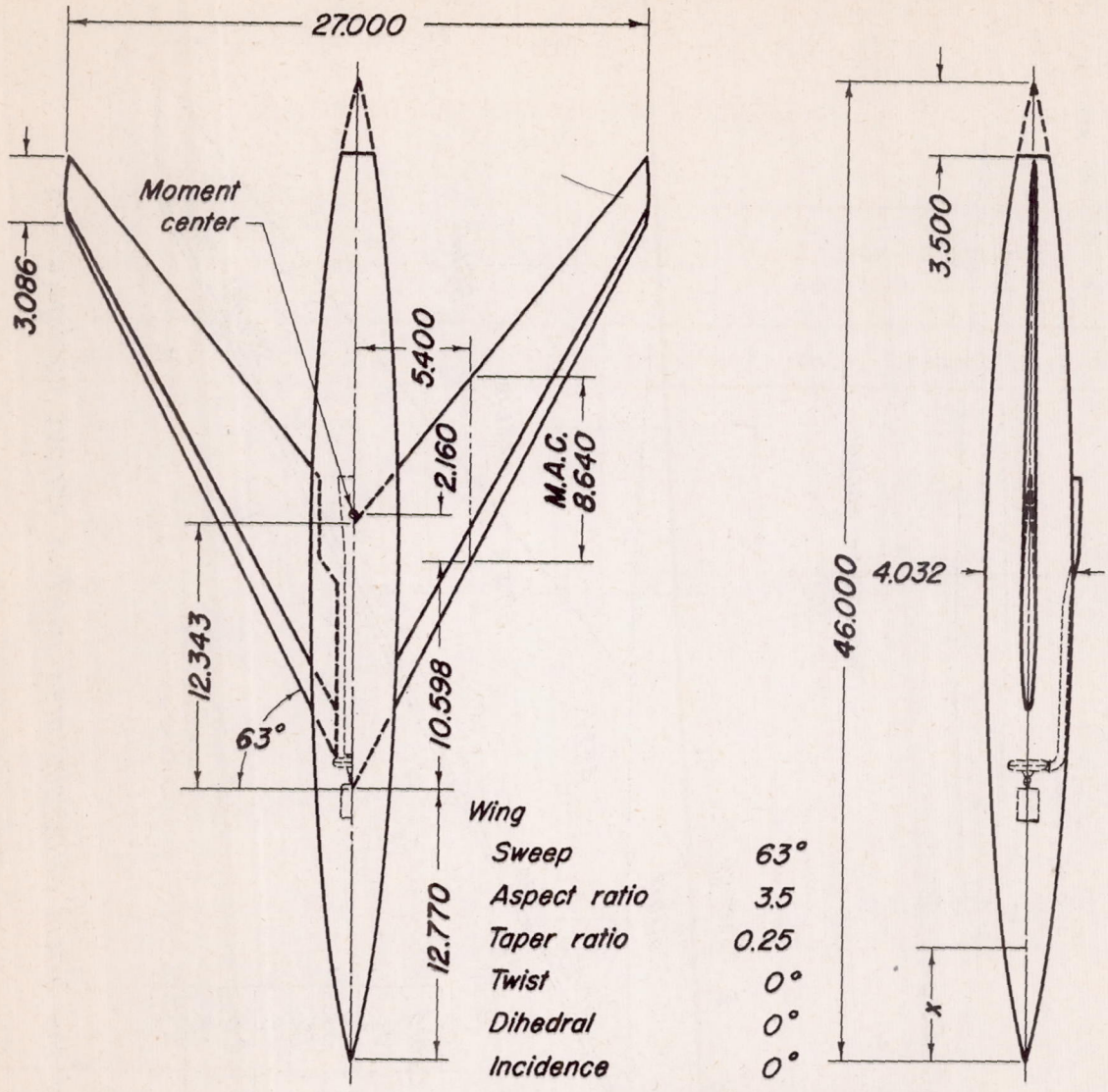

Wing	
Sweep	63°
Aspect ratio	3.5
Taper ratio	0.25
Twist	0°
Dihedral	0°
Incidence	0°
Airfoil section	NACA 64A006
Area	208.3 sq ft
Fuselage	
Fineness ratio	10.5
Radius at station x	$2.016\left(1-\left(\frac{x}{23}-1\right)^2\right)^{3/4}$ ft

All dimensions in feet unless otherwise noted.

NACA

Figure 1.—Geometric characteristics of the 63° swept-back wing with fuselage.

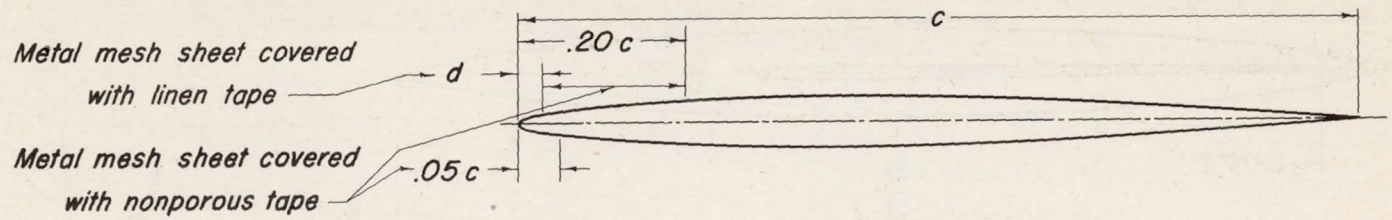

Streamwise section

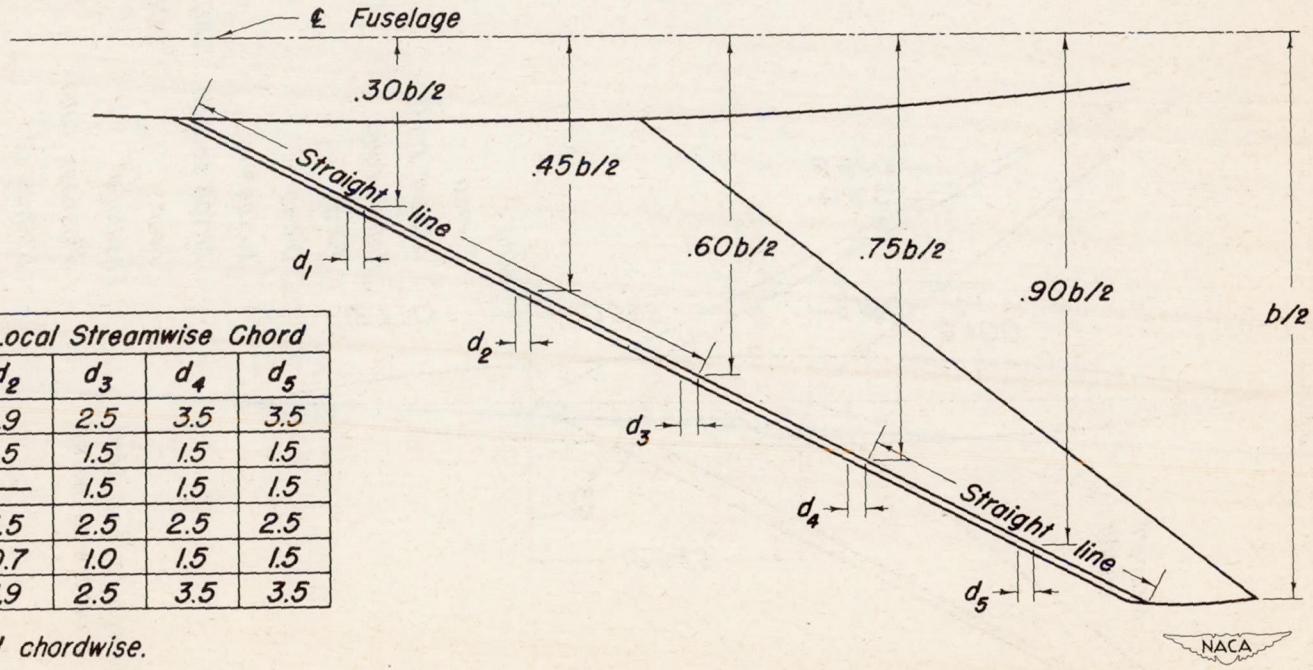

Model Configuration	Percent Local Streamwise Chord				
	d_1	d_2	d_3	d_4	d_5
A	1.5	1.9	2.5	3.5	3.5
B	1.5	1.5	1.5	1.5	1.5
C	—	—	1.5	1.5	1.5
D	1.0	1.5	2.5	2.5	2.5
E	0.5	0.7	1.0	1.5	1.5
F[1]	1.5	1.9	2.5	3.5	3.5

[1]Porosity varied chordwise.

Figure 2.—Schematic drawing of the extent of porous area used in various configurations.

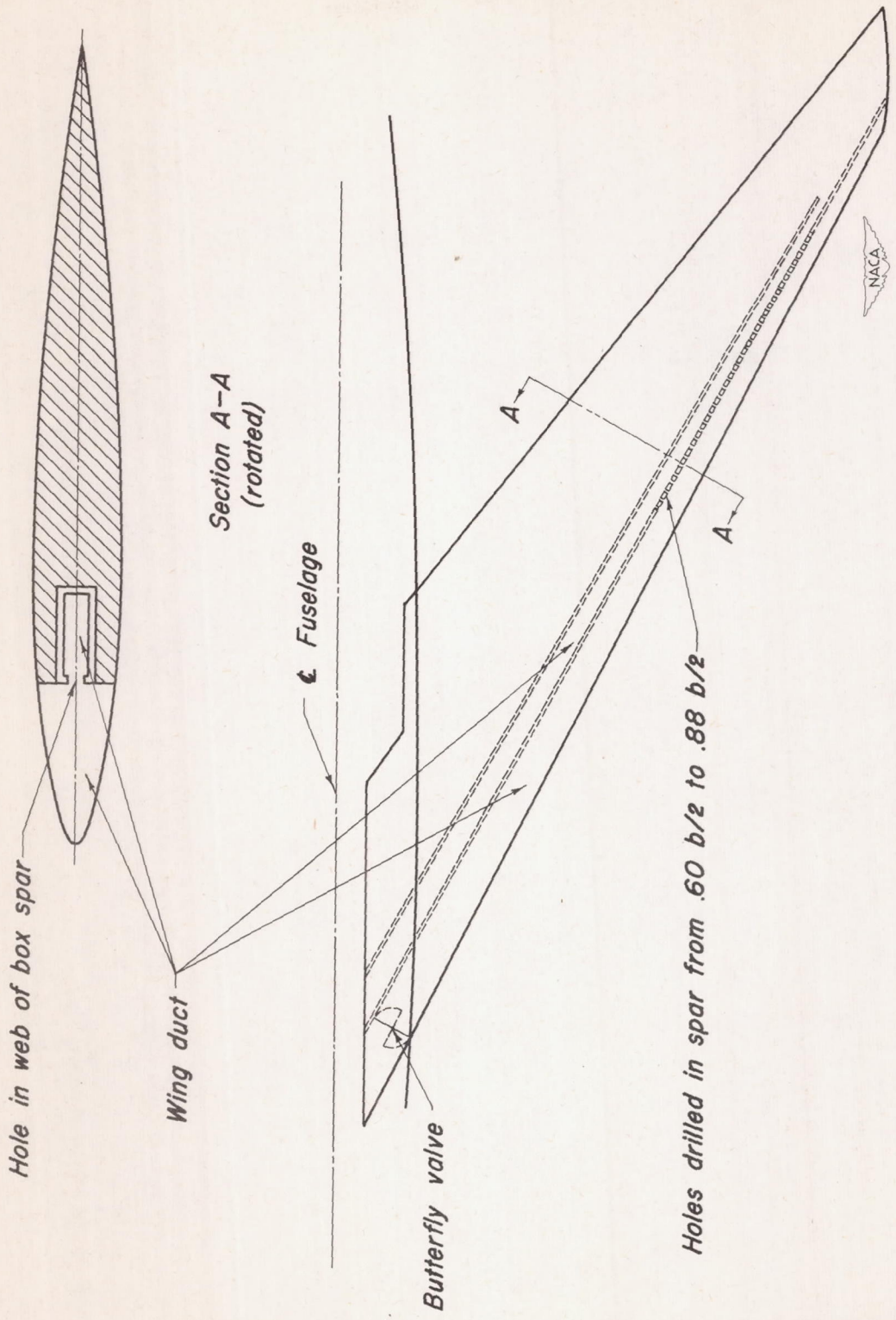

Figure 3.—Schematic drawing of the air ducts within the wing.

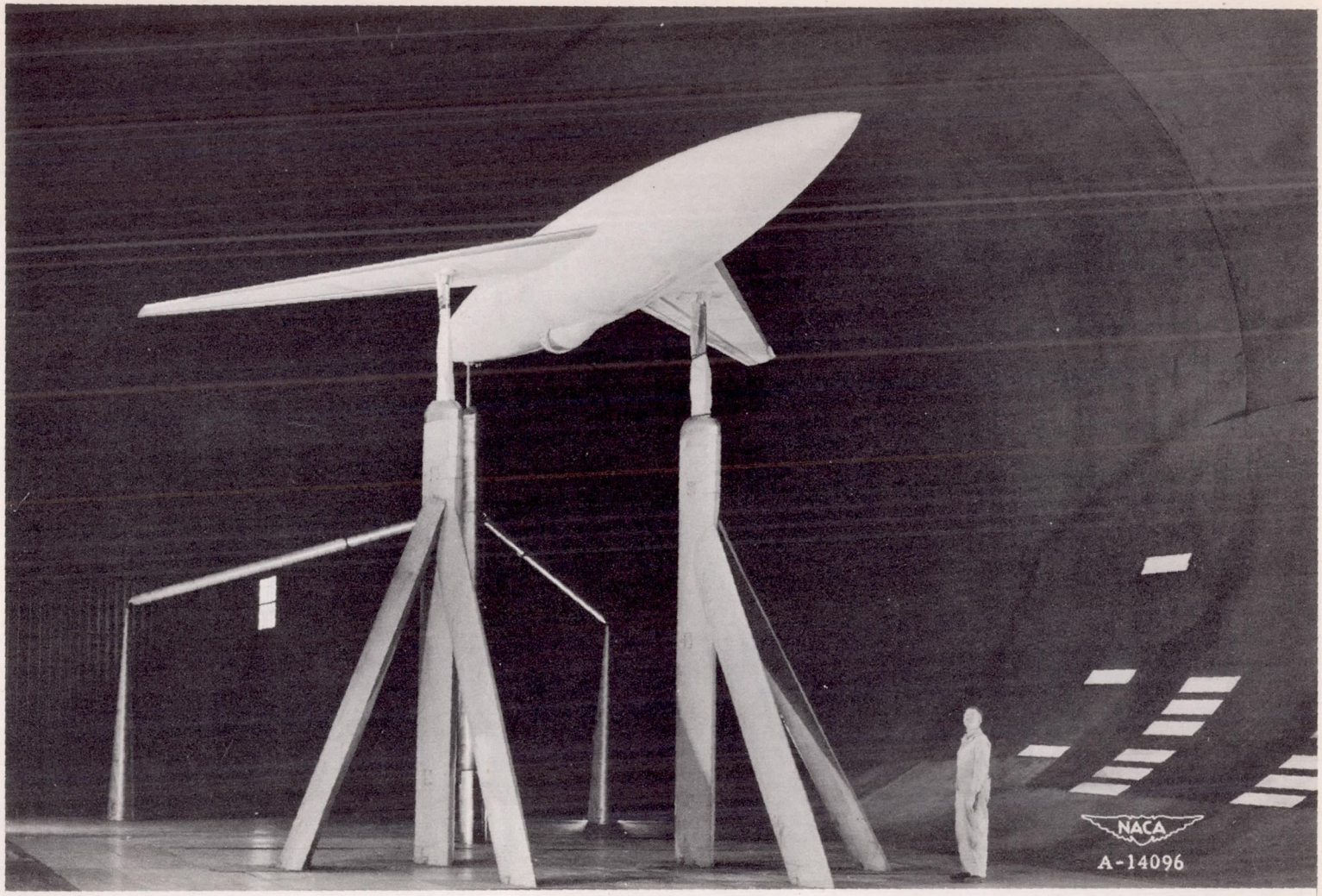

Figure 4.- The 63° swept-back wing with fuselage mounted in the Ames 40- by 80-foot wind tunnel.

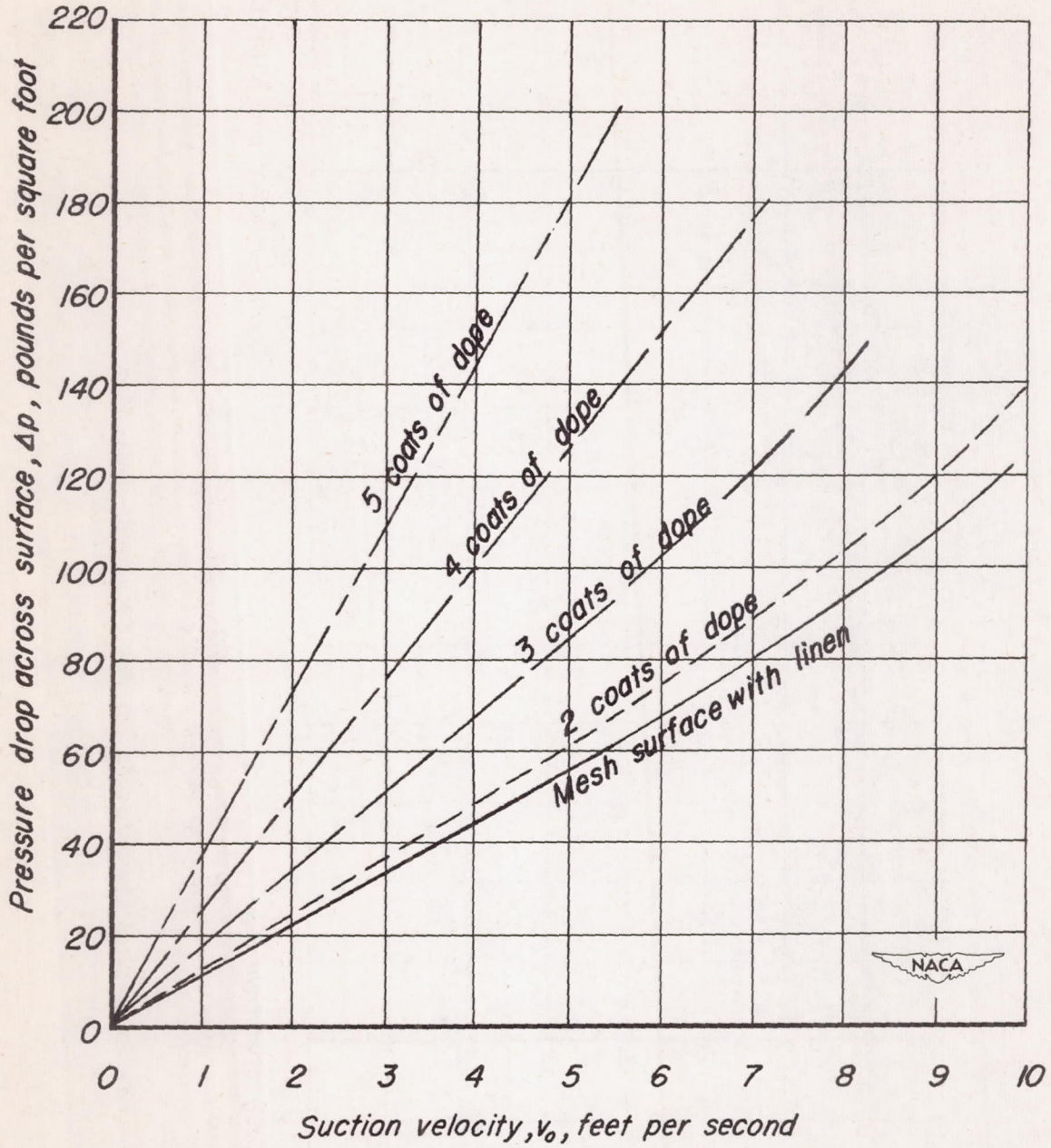

Figure 5 .—Calibration of suction-air velocities for various porous surfaces with no tangential velocities on the outer surface.

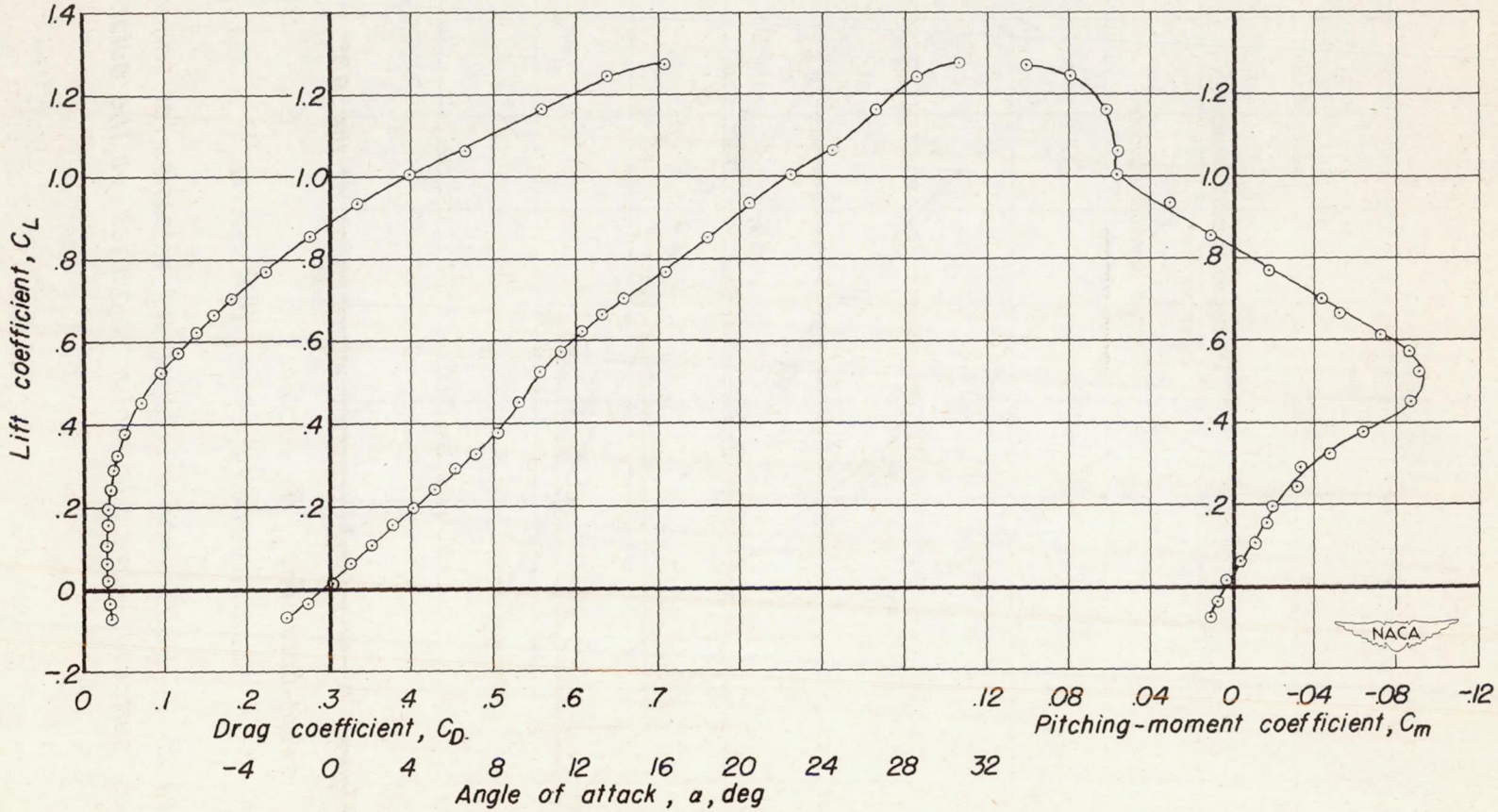

Figure 6.— The longitudinal characteristics of the 63° swept-back wing.

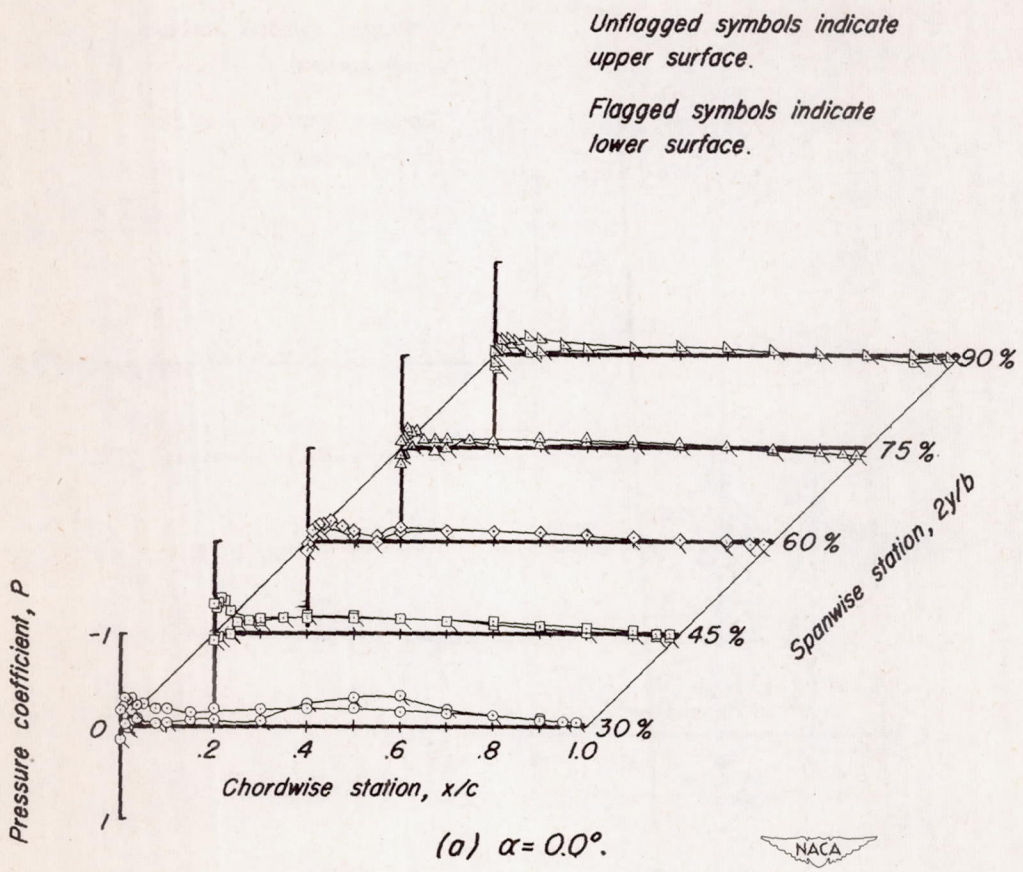

Figure 7.—Chordwise pressure distributions of the 63° swept-back wing. No suction.

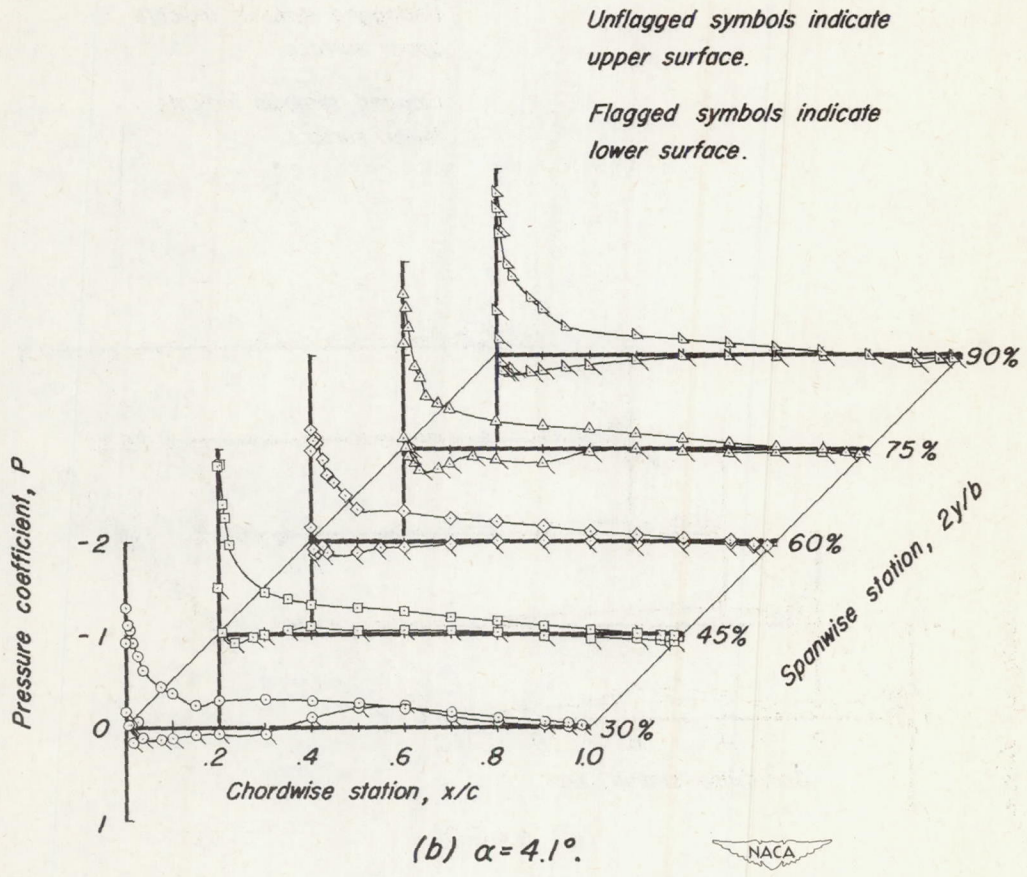

Figure 7.— Continued.

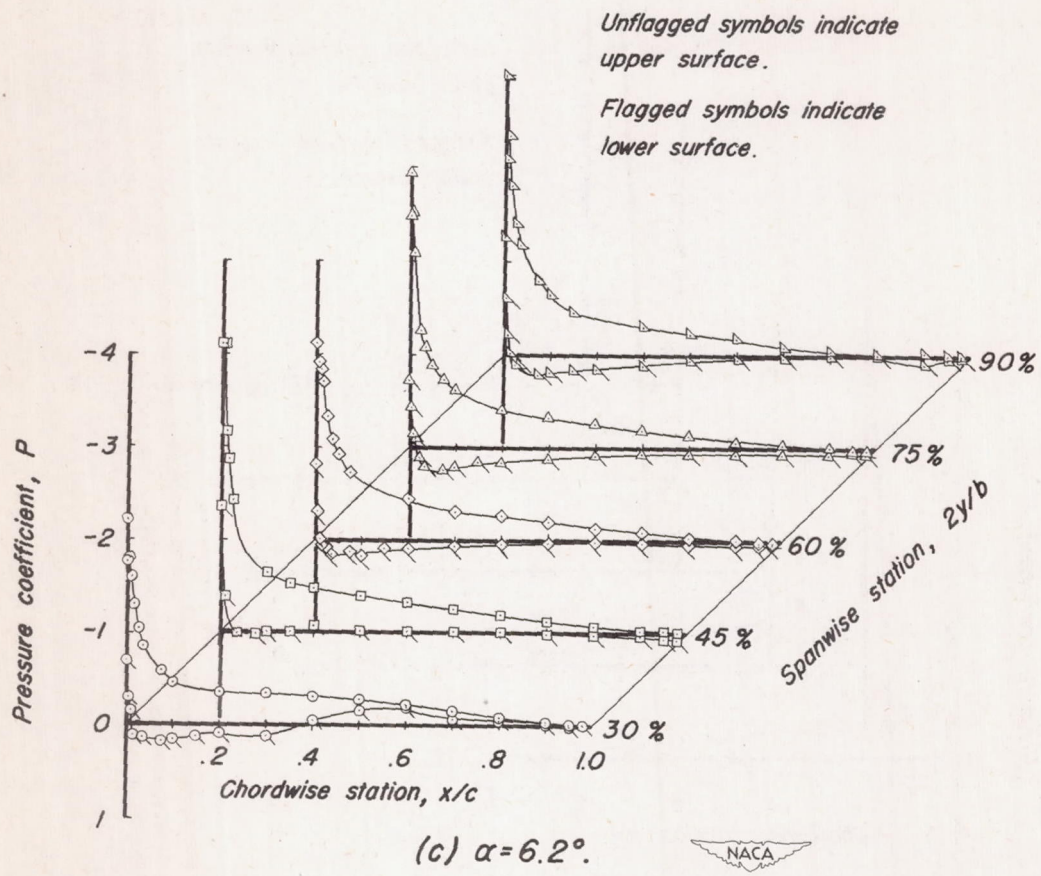

Figure 7.—Continued.

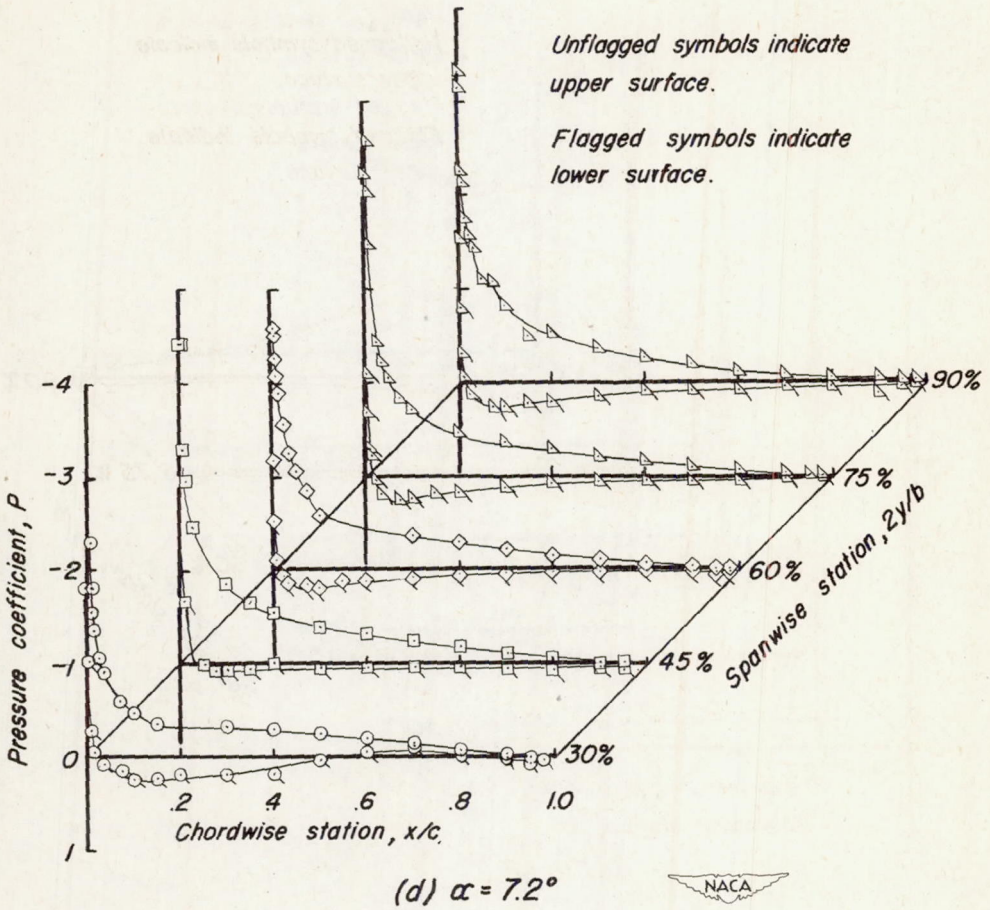

Figure 7.— Continued.

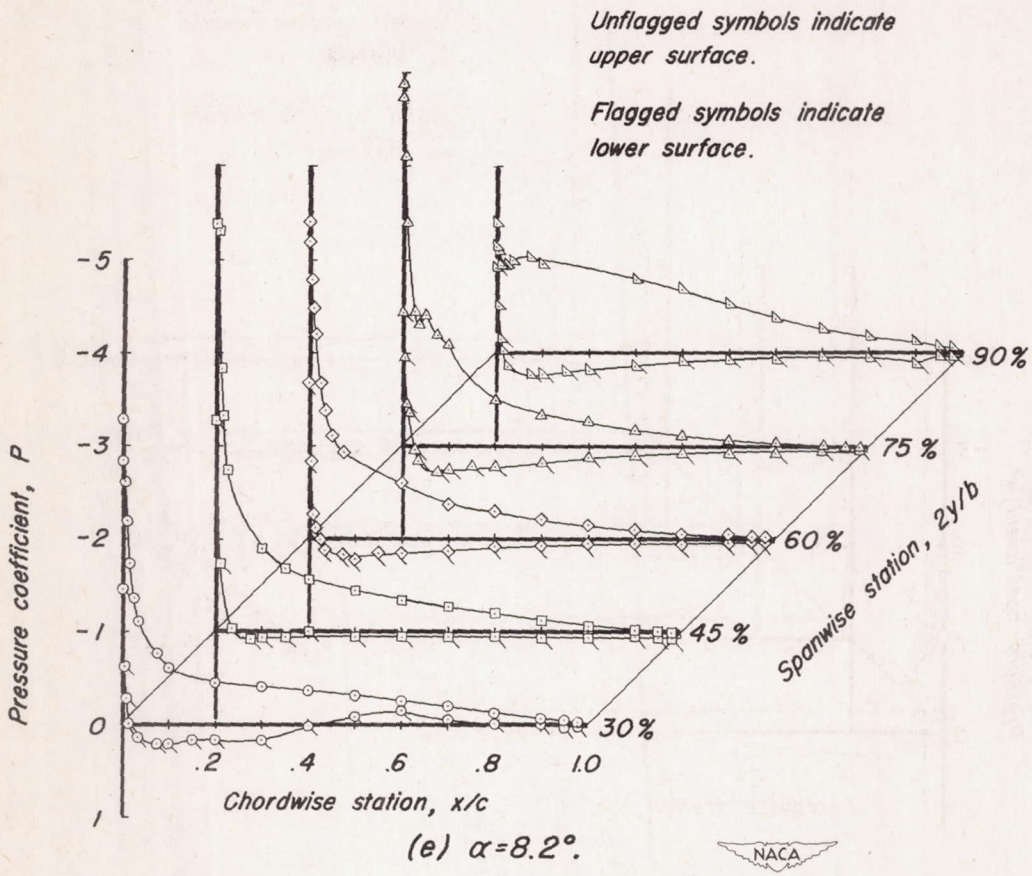

Figure 7.—Continued.

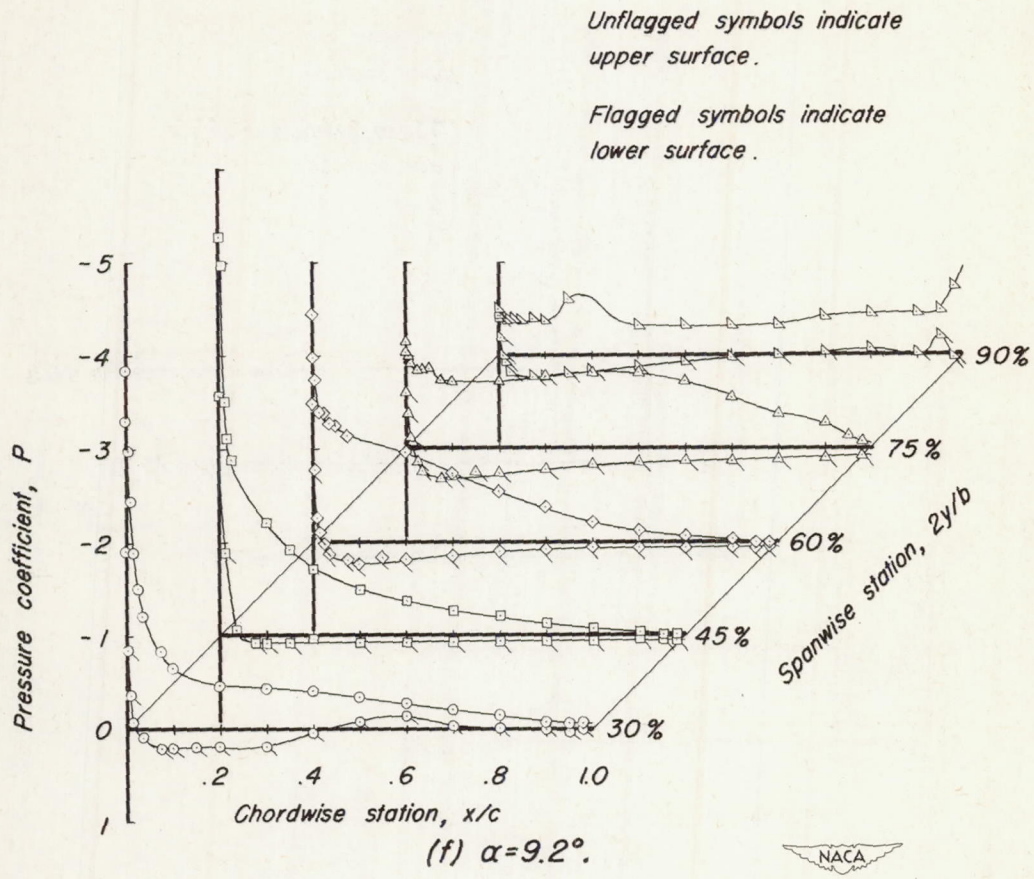

Figure 7.—Continued.

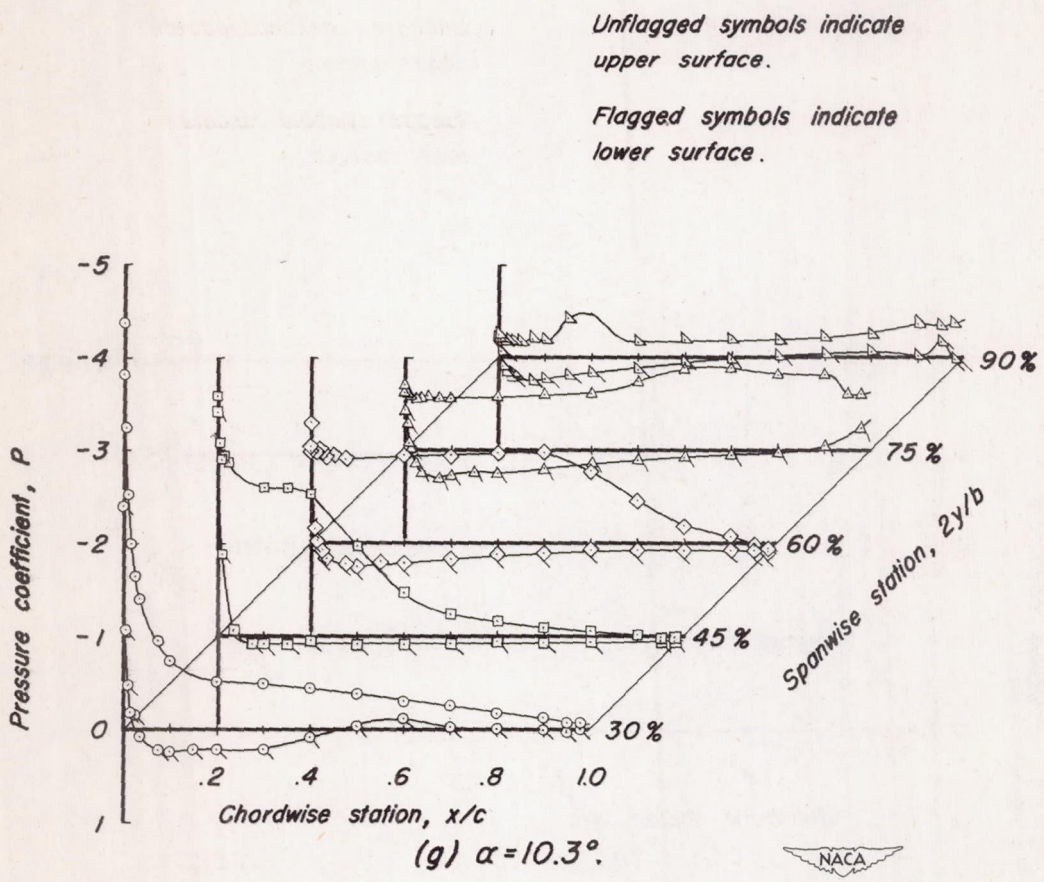

Figure 7.—Continued.

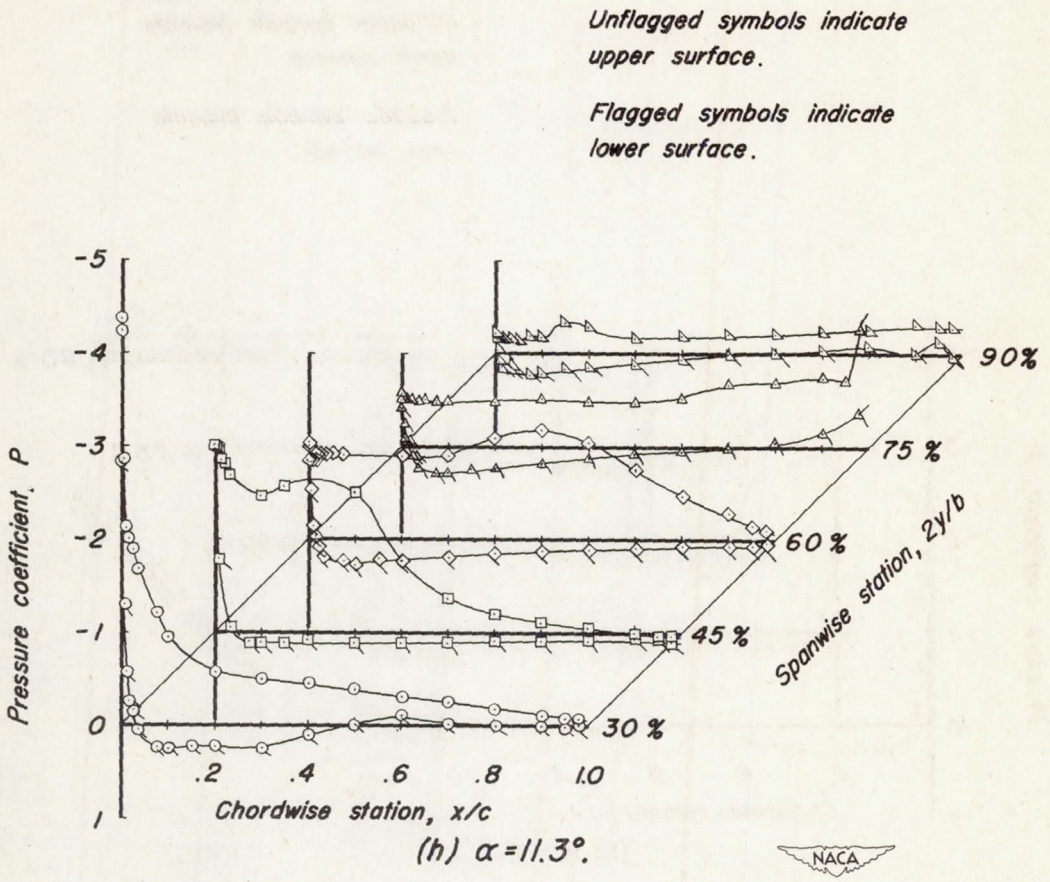

Figure 7.—Continued.

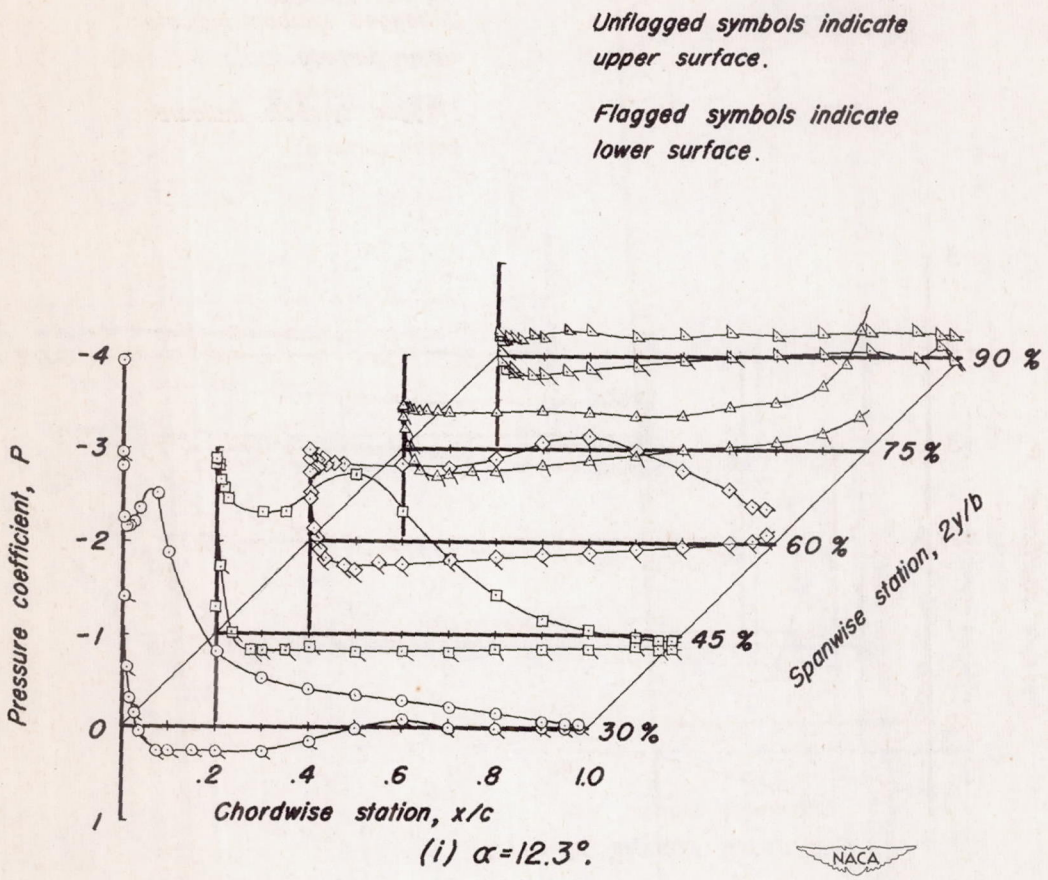

Figure 7.—Continued.

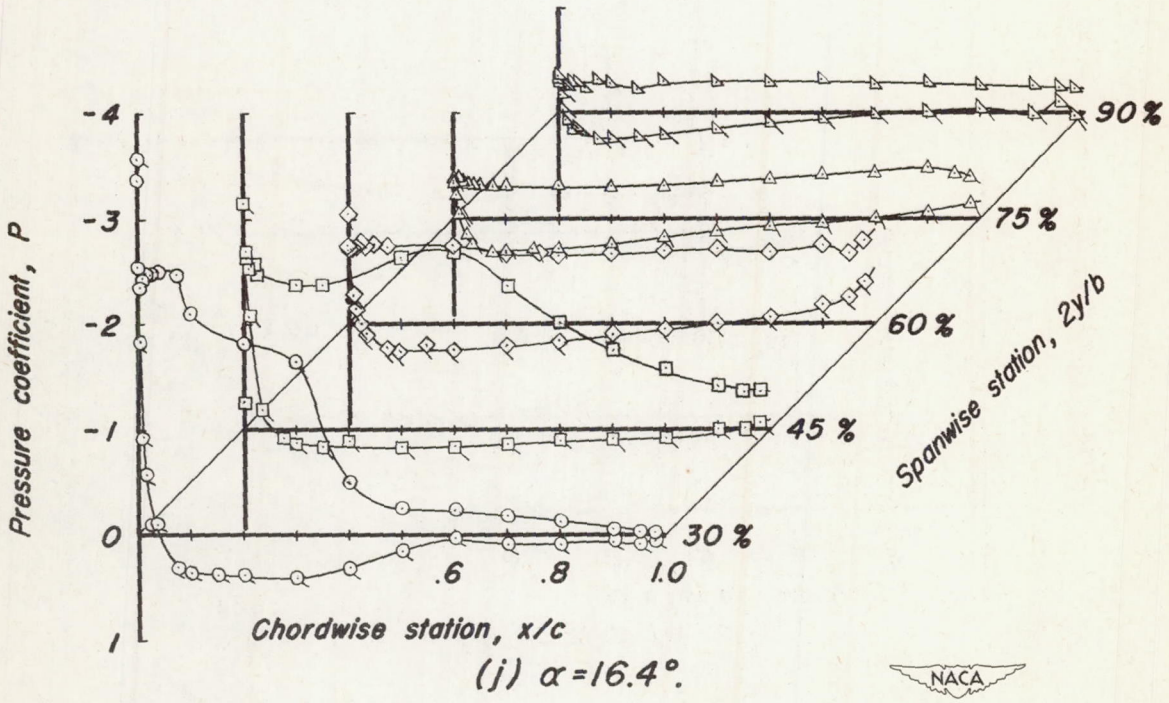

Figure 7.—Continued.

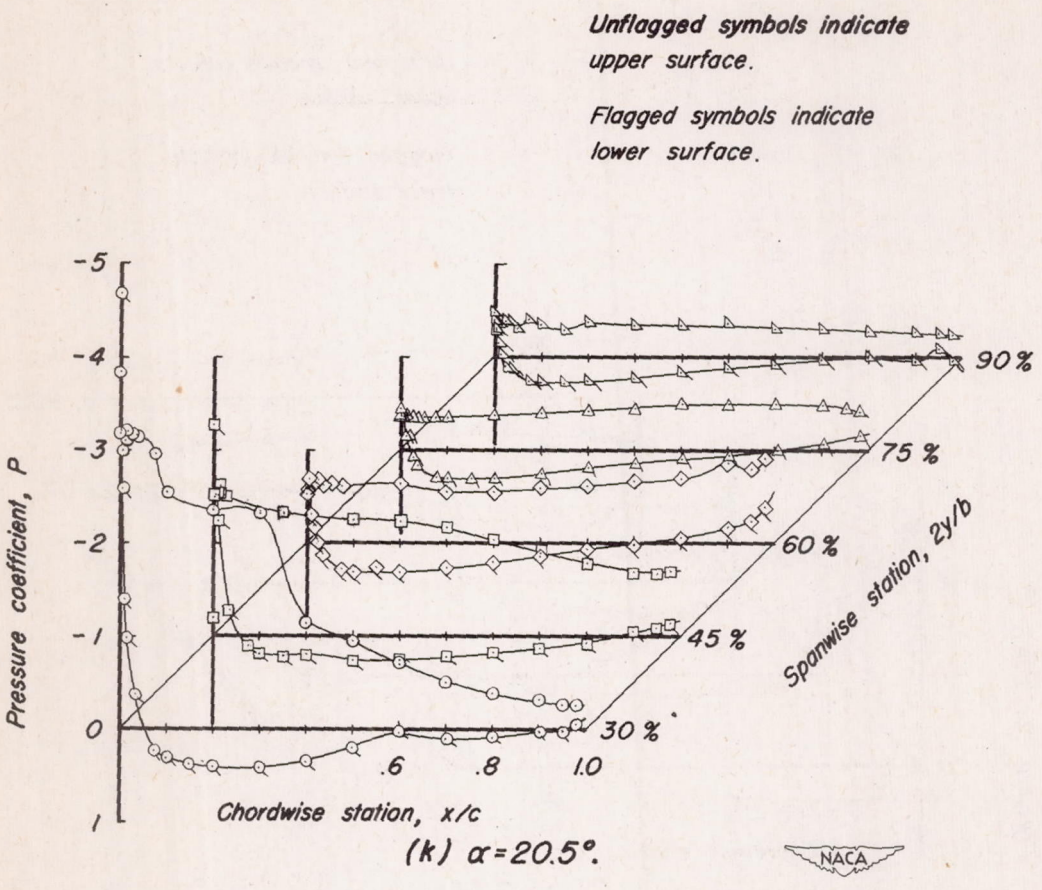

Figure 7.—Continued.

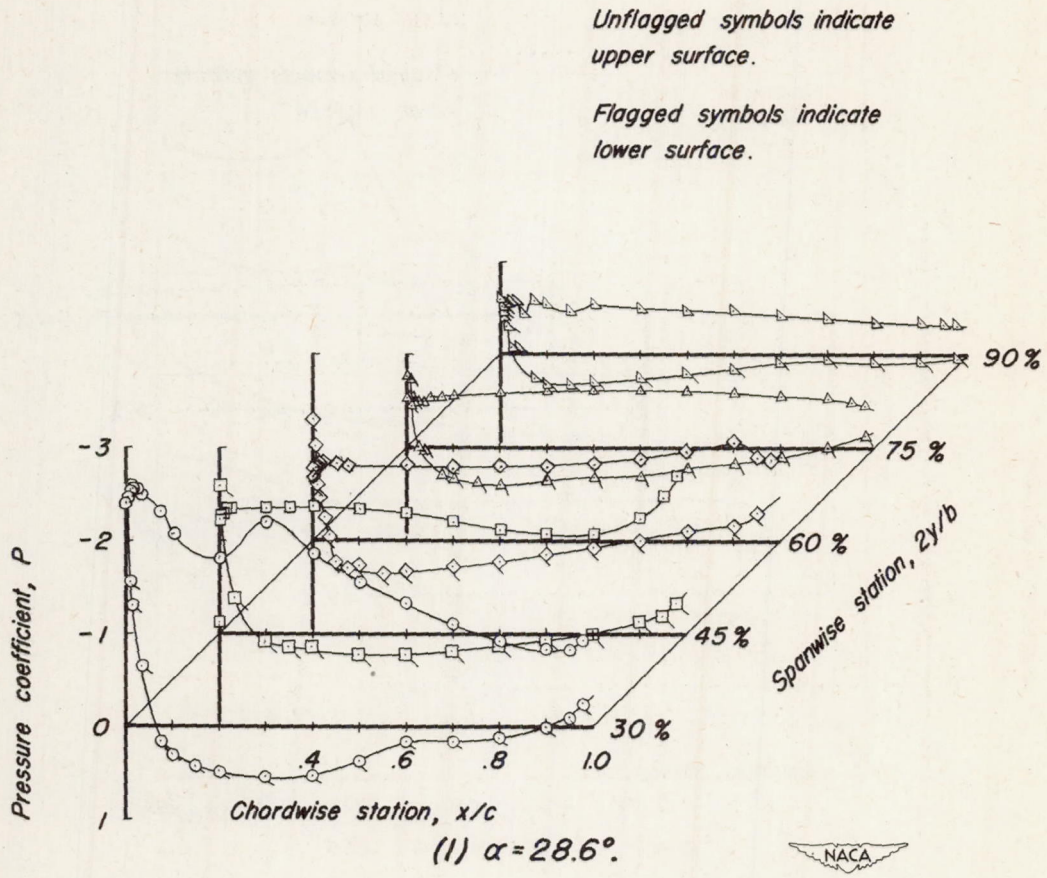

Figure 7.—Concluded.

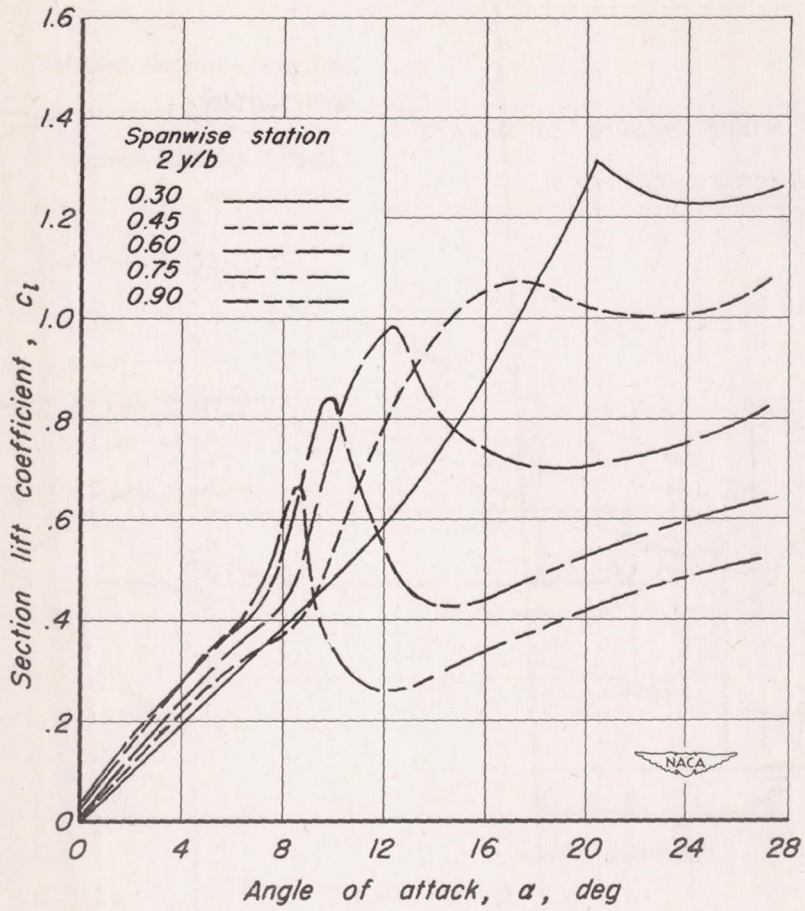

Figure 8.- Section lift curves of the 63° swept-back wing. No suction.

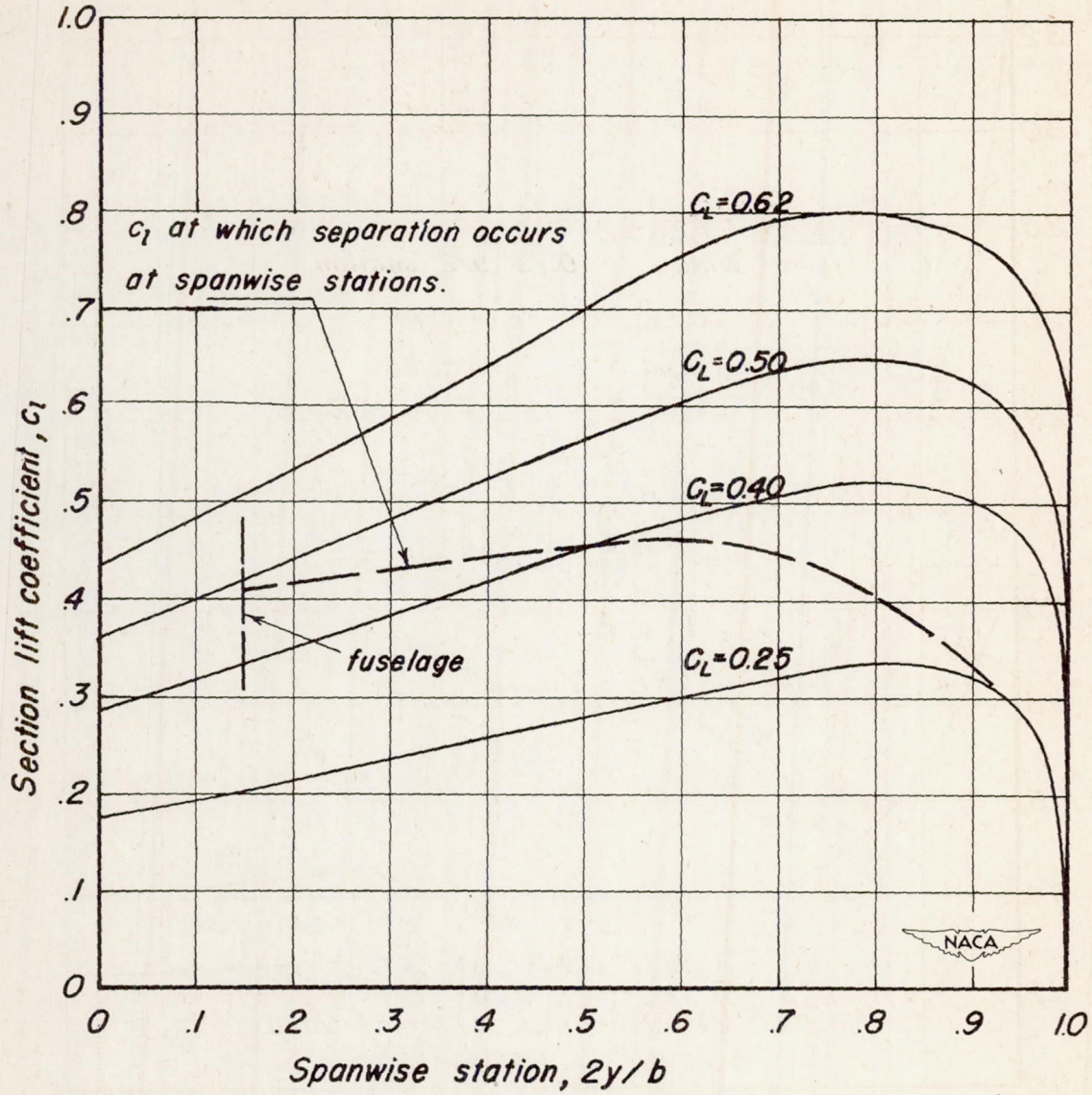

Figure 9.— Curves used to estimate the spanwise extent of porous area for various lift coefficients on the 63° swept-back wing.

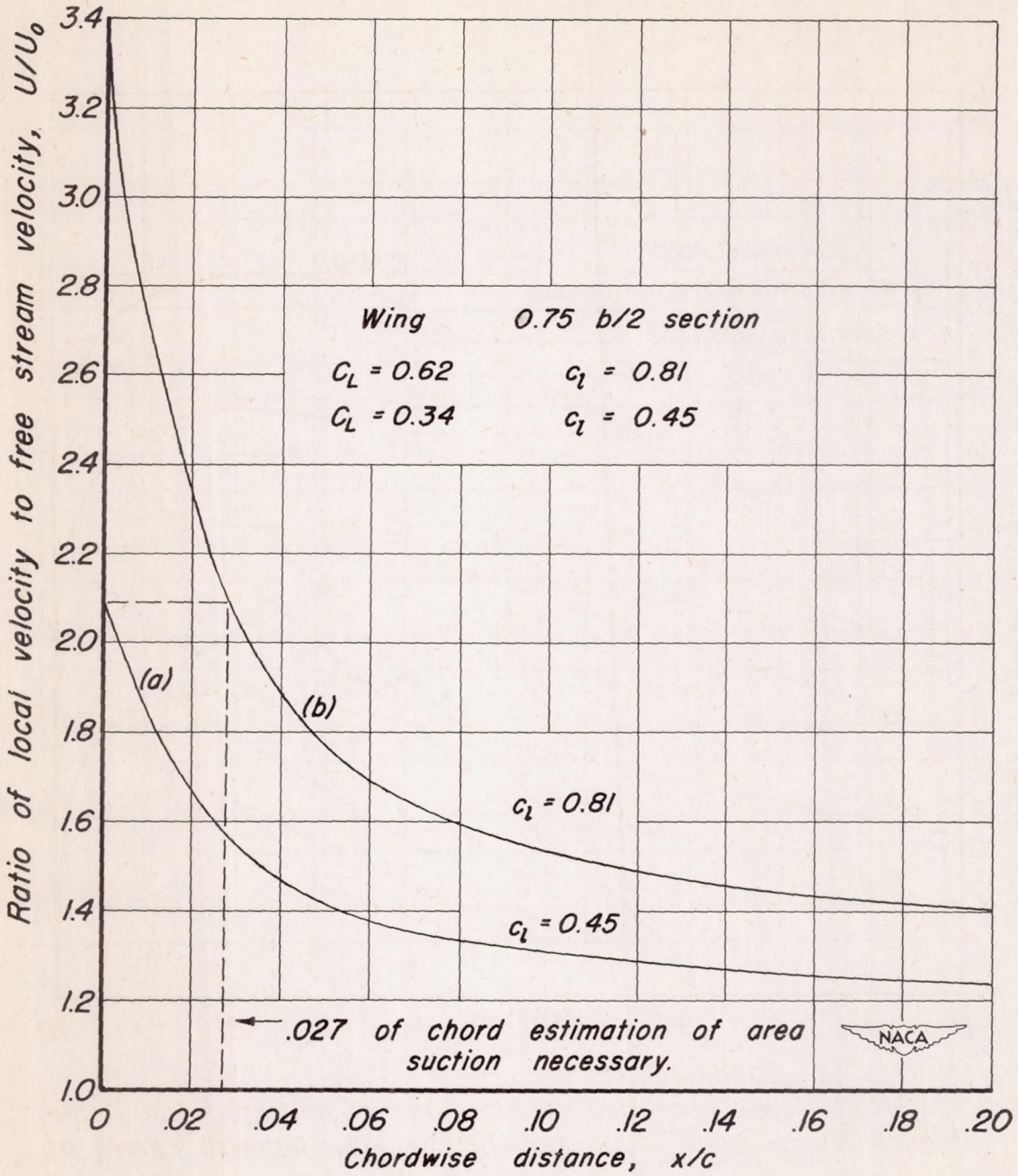

Figure 10.-Curves used to estimate the chordwise extent of area at the individual sections on the 63° swept-back wing.

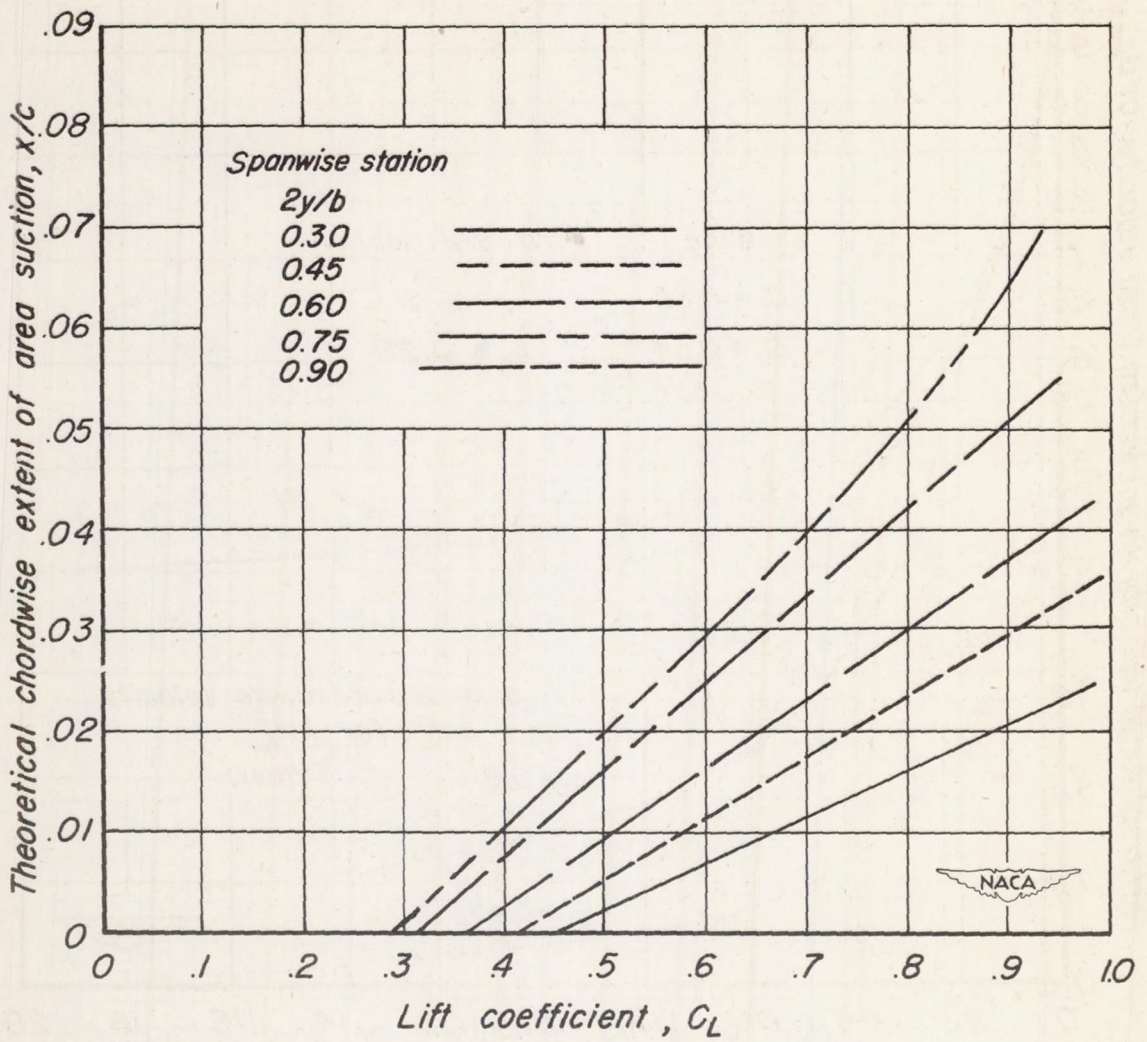

Figure 11.—Theoretical estimations of the chordwise extent of area suction required to maintain unseparated flow on the 63° swept-back wing at the various spanwise stations.

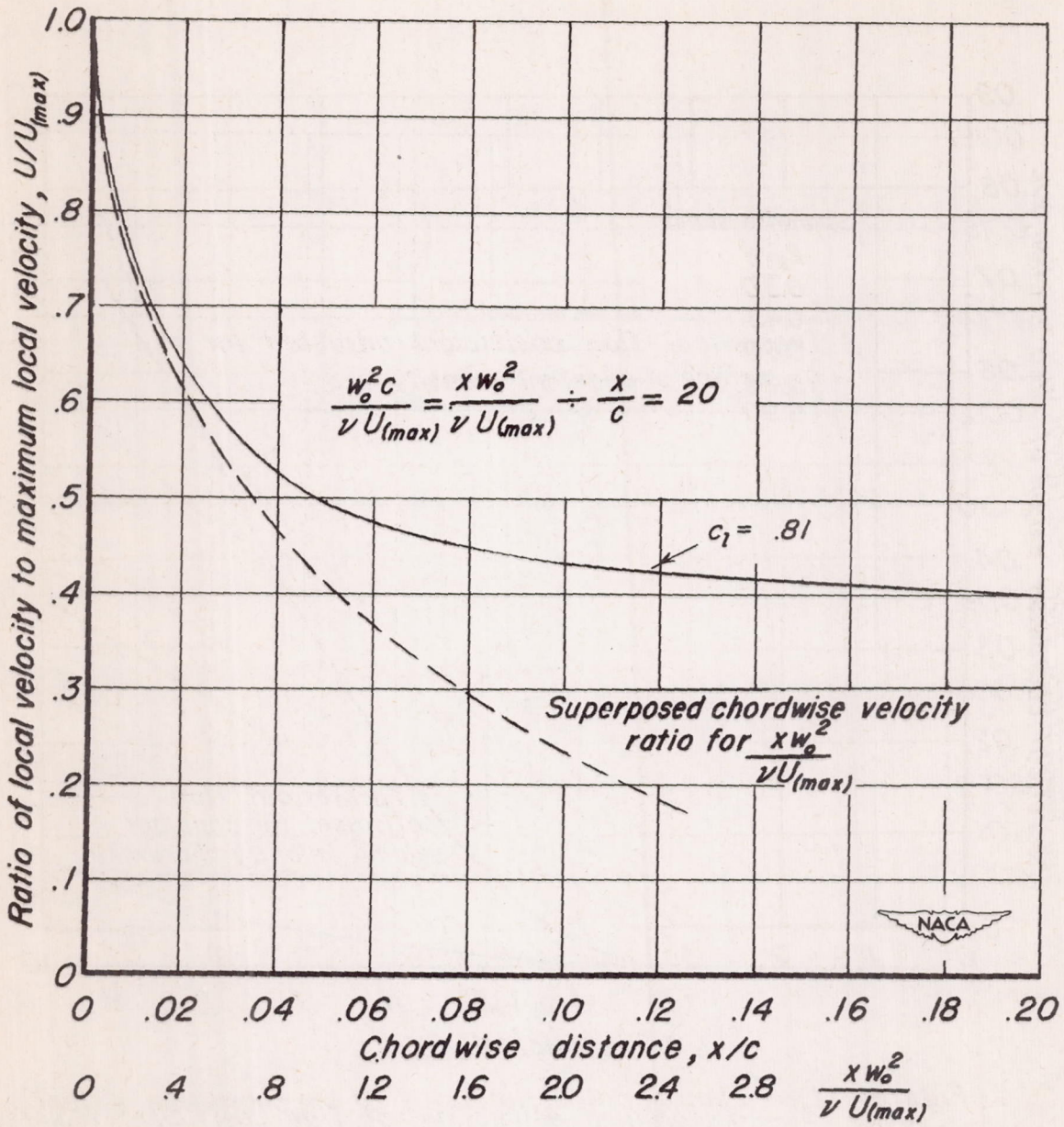

Figure 12.— Curves used to estimate the suction-air velocity necessary to maintain a boundary layer similar to a Blasius' profile in a certain velocity distribution.

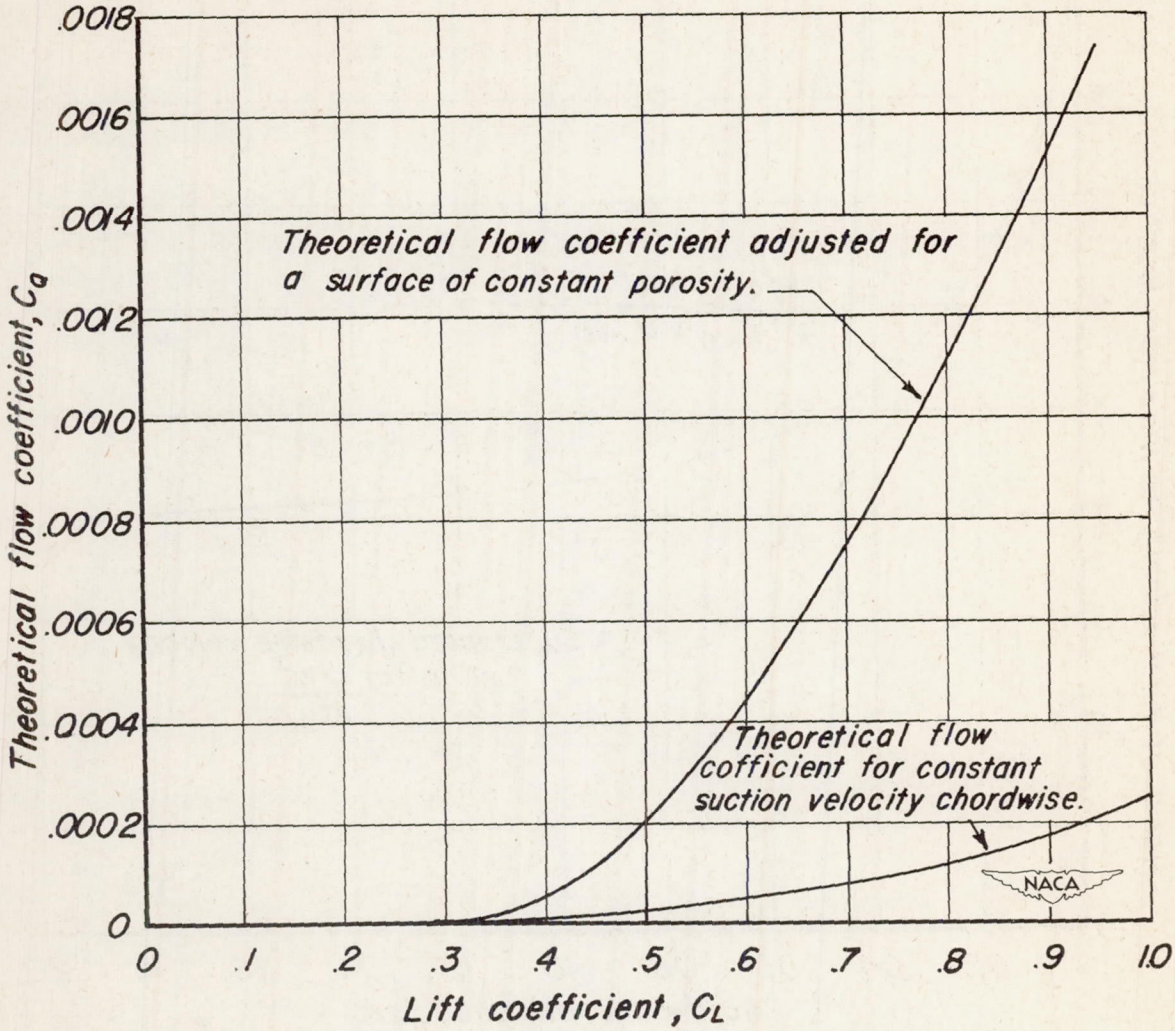

Figure 13.—Theoretical estimations of flow coefficient required for the 63° swept-back wing for a range of lift coefficients.

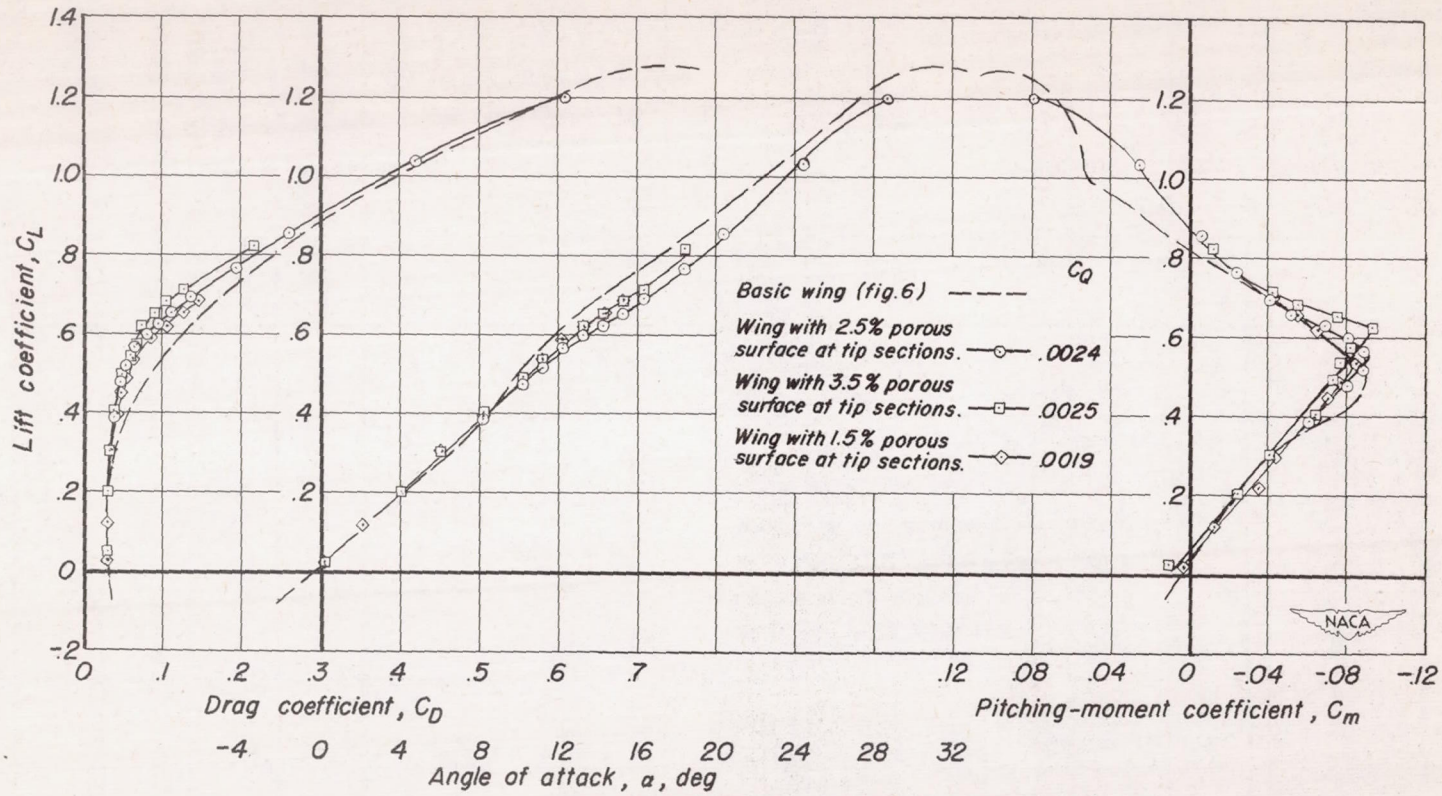

(a) Configurations D, A & B.

Figure 14.— Effect of variation of the porous surface chordwise on the longitudinal characteristics of the 63° swept-back wing with full-span application of area suction.

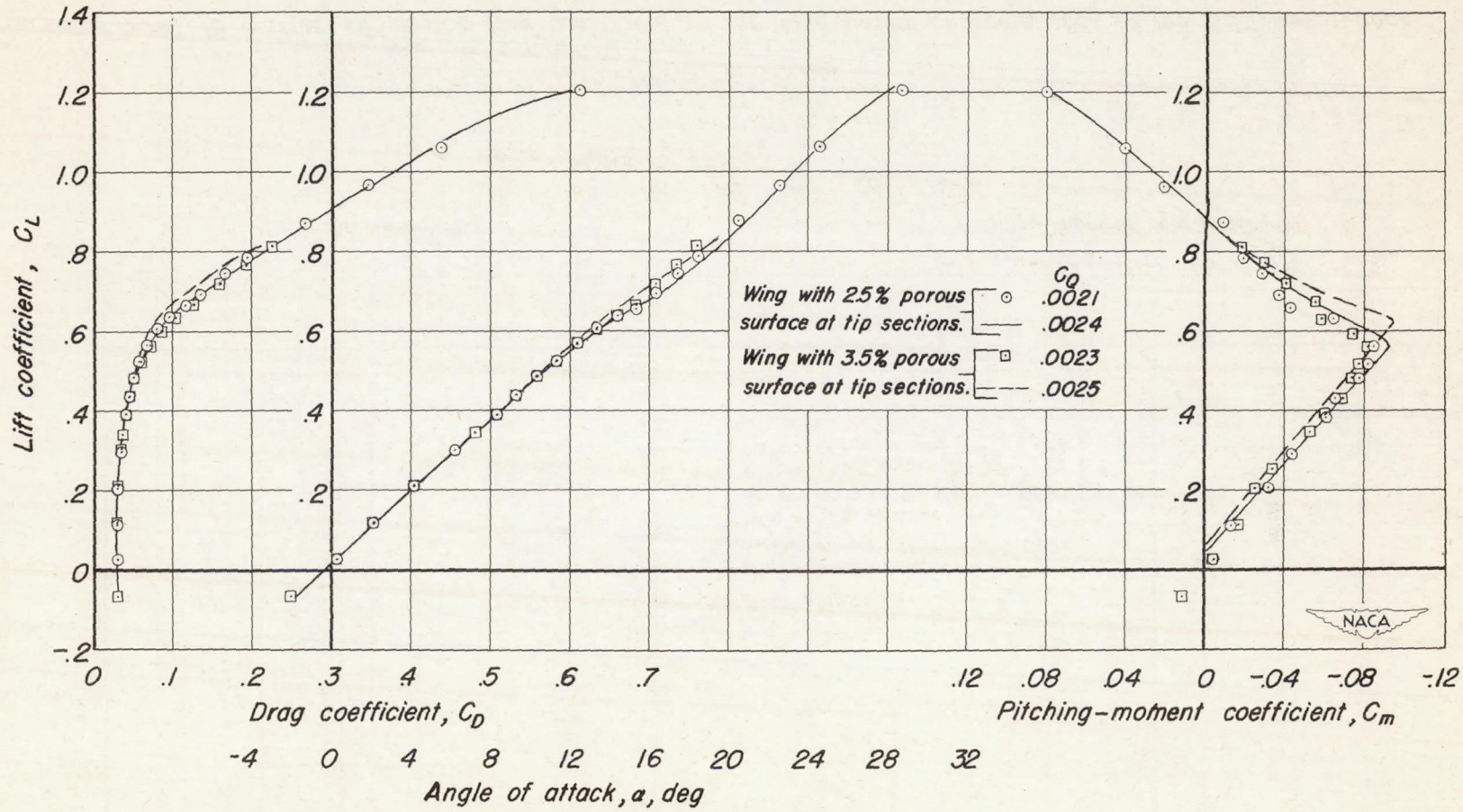

(b) Configurations A&D.

Figure 14.—Concluded.

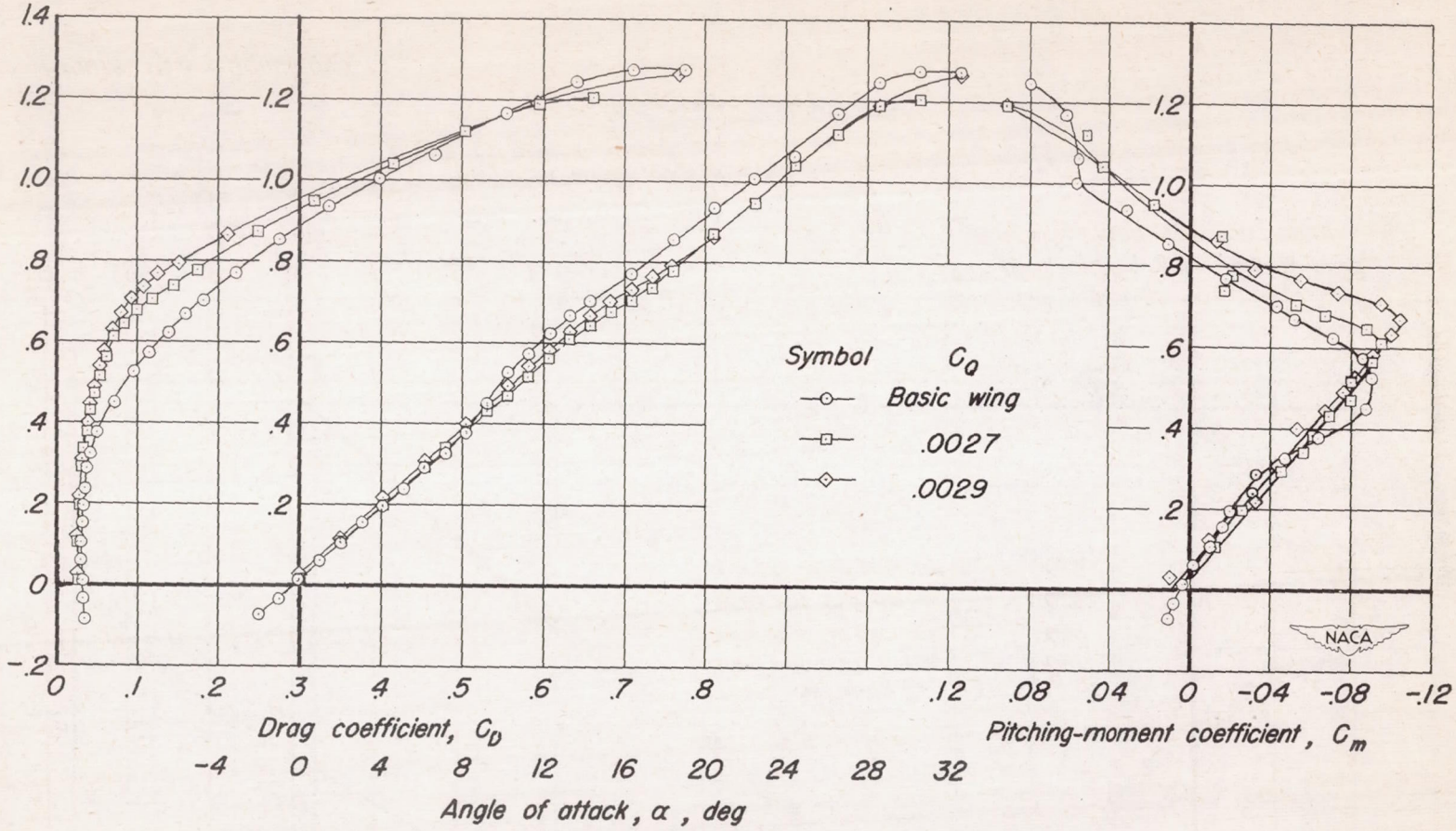

(a) C_Q = 0.0027 & 0.0029.

Figure 15.—Effect of varying flow coefficient on the longitudinal characteristics of the 63° swept-back wing with fuselage. Configuration A.

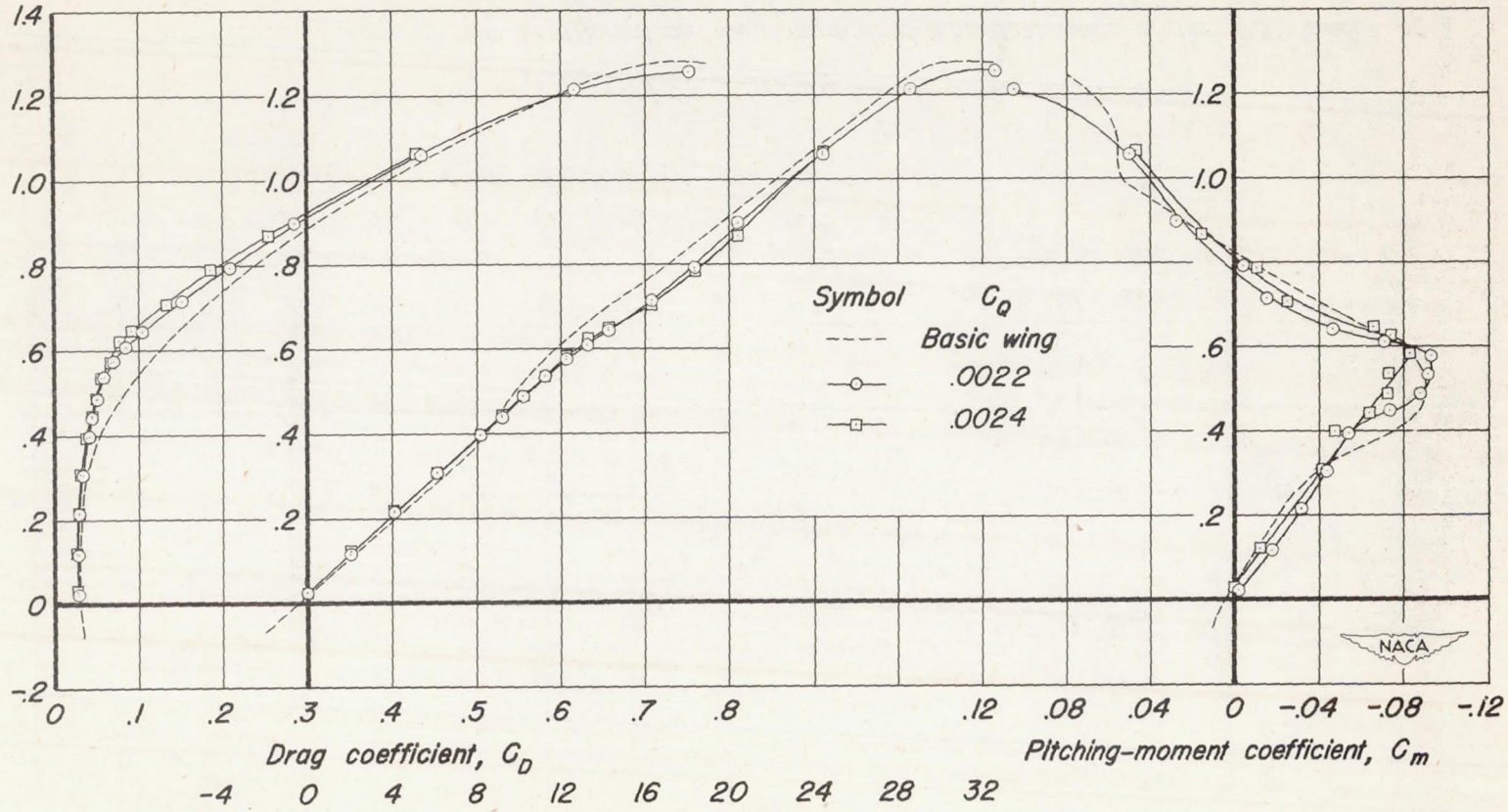

(b) C_Q = 0.0022 & 0.0024.

Figure 15.—Concluded.

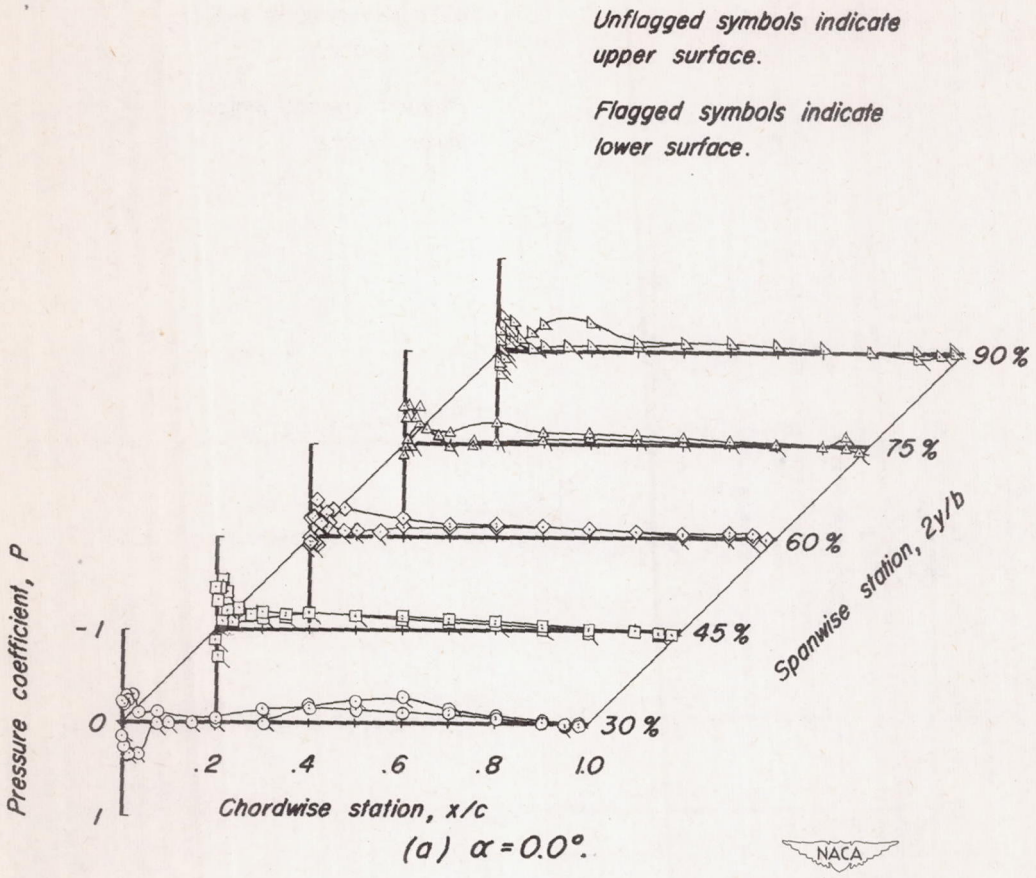

Figure 16.—Chordwise pressure distributions of the 63° swept-back wing with area suction. $C_Q = 0.0029$. Configuration A.

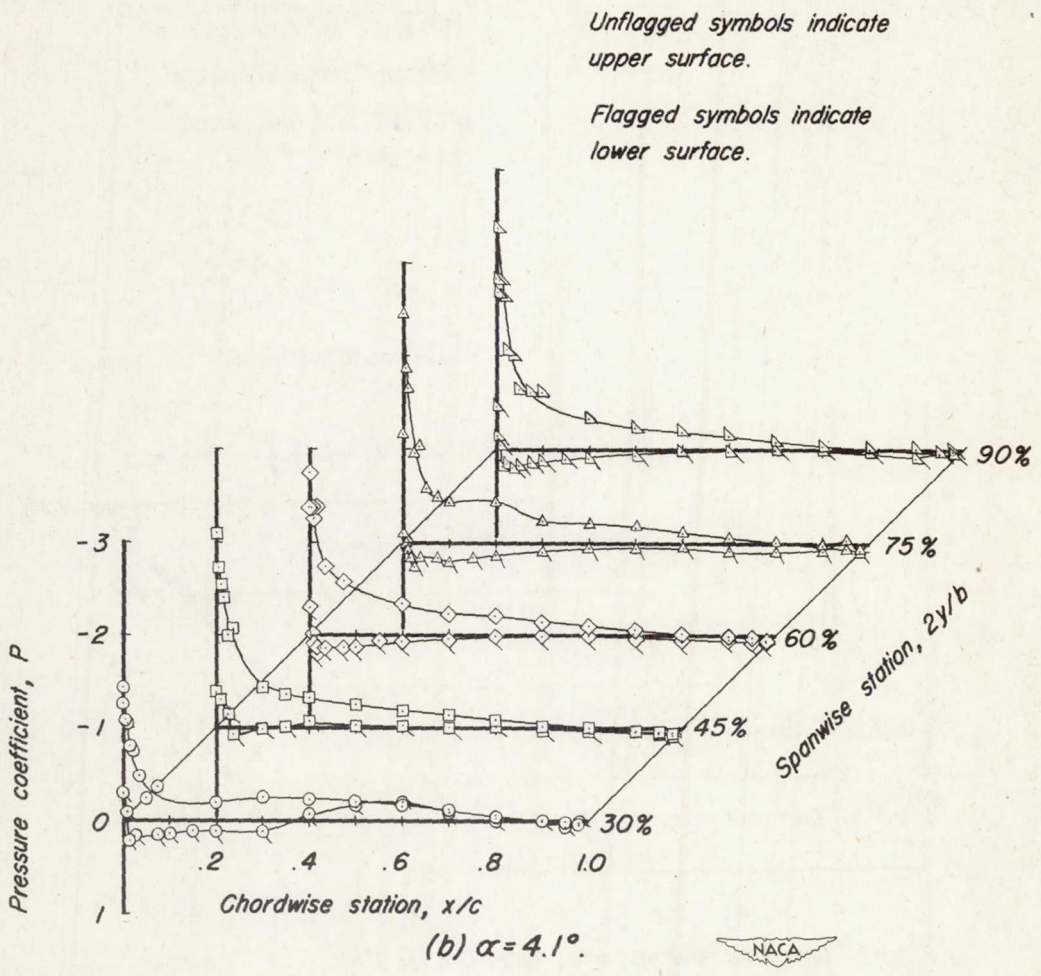

Figure 16.—Continued.

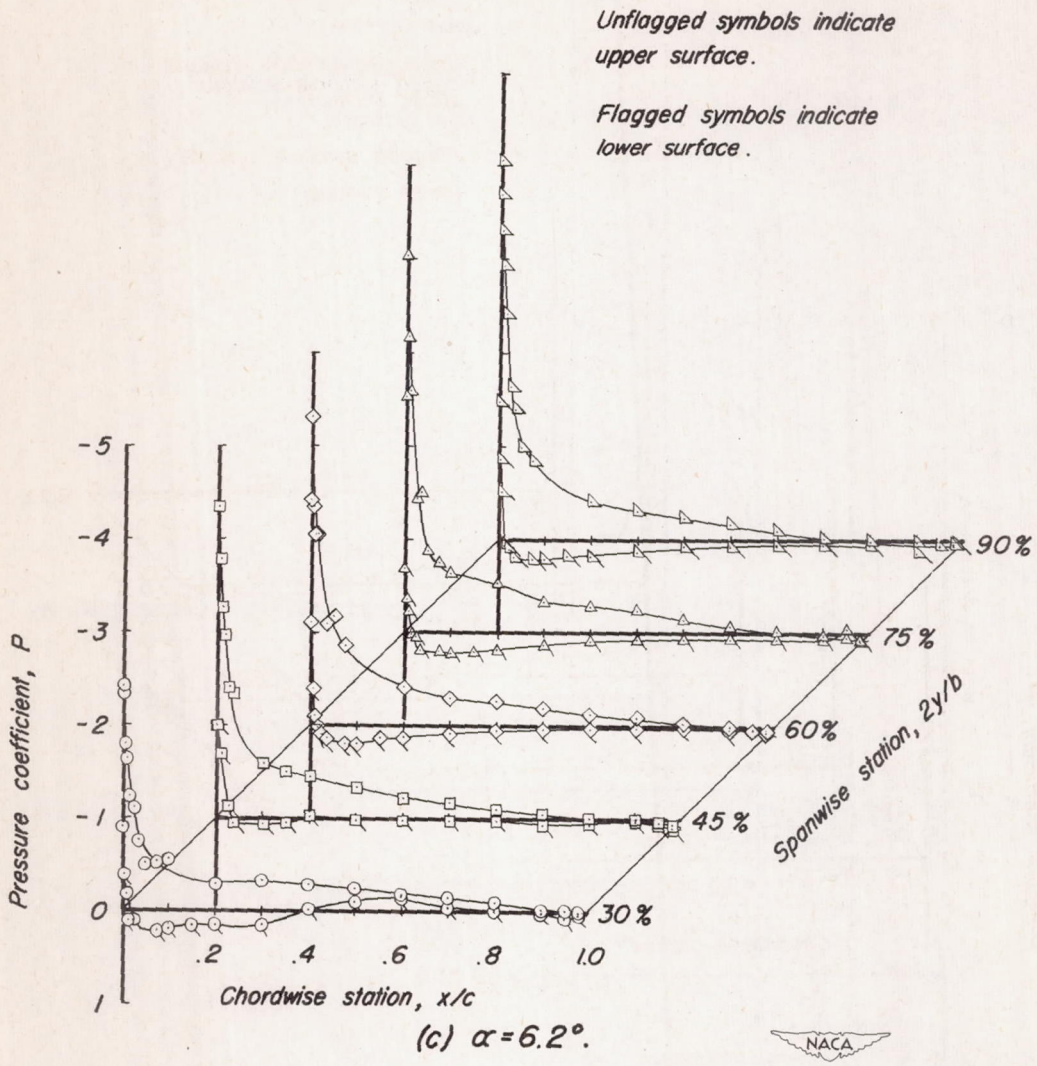

Figure 16.-Continued.

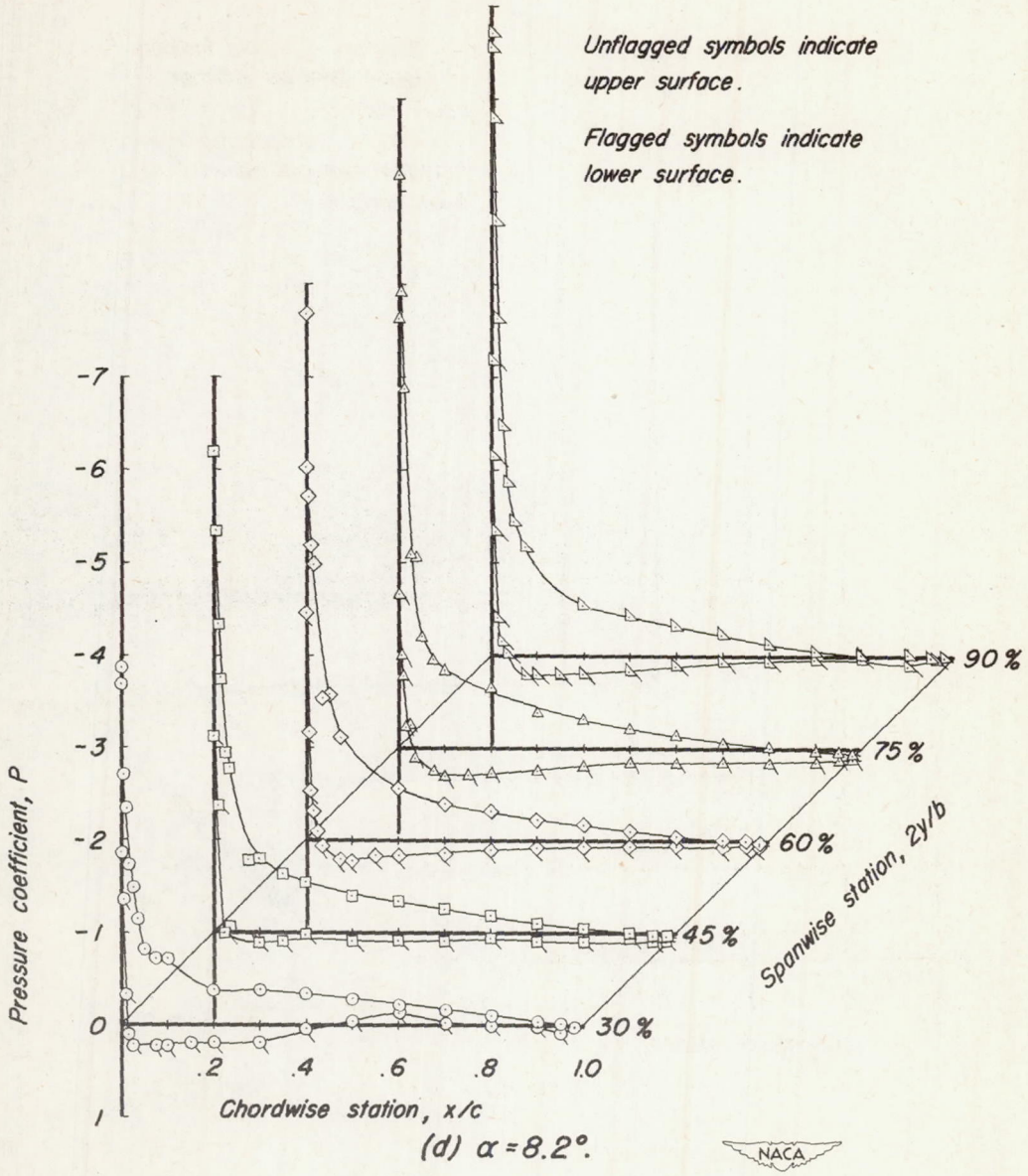

Figure 16.–Continued.

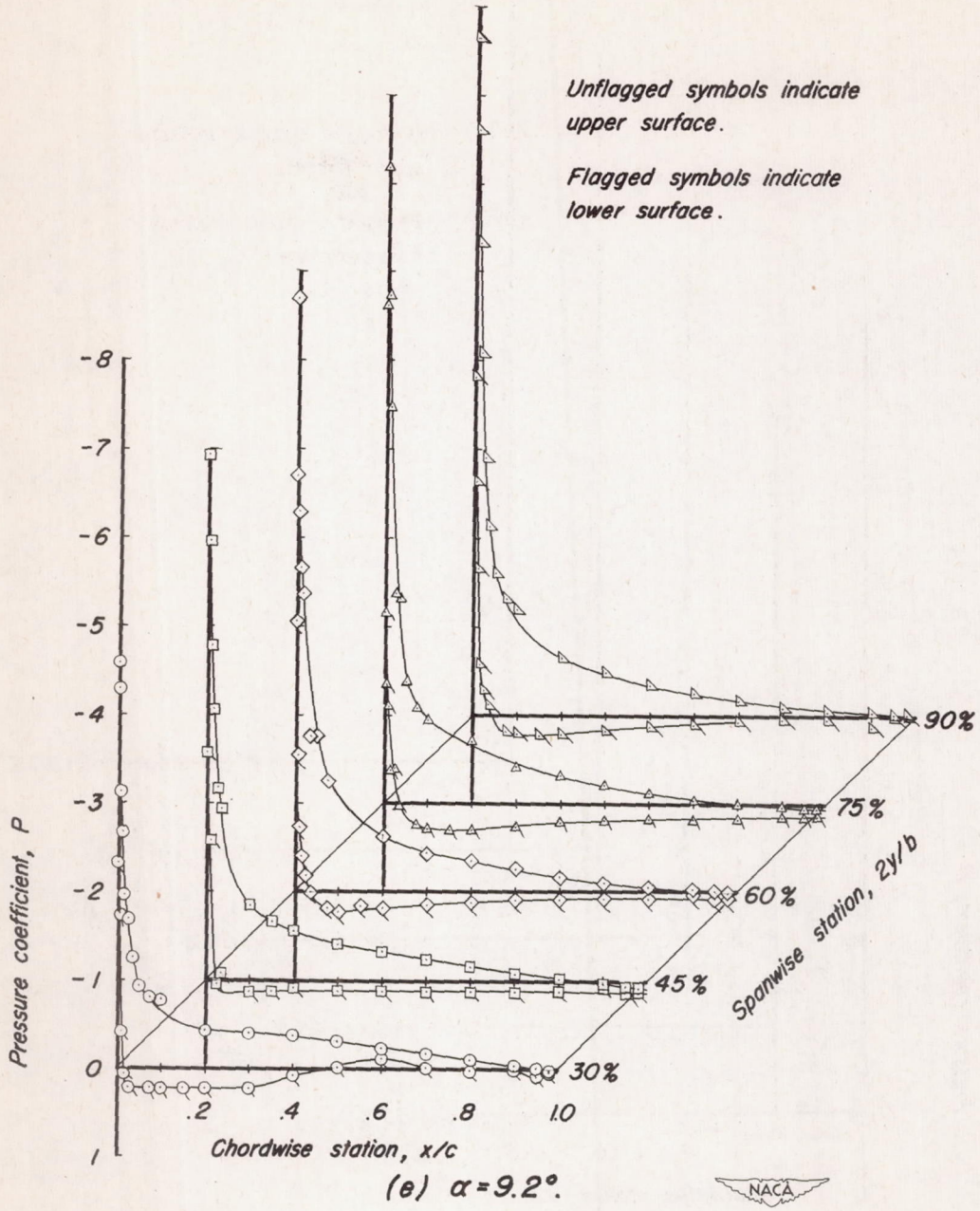

Figure 16.—Continued.

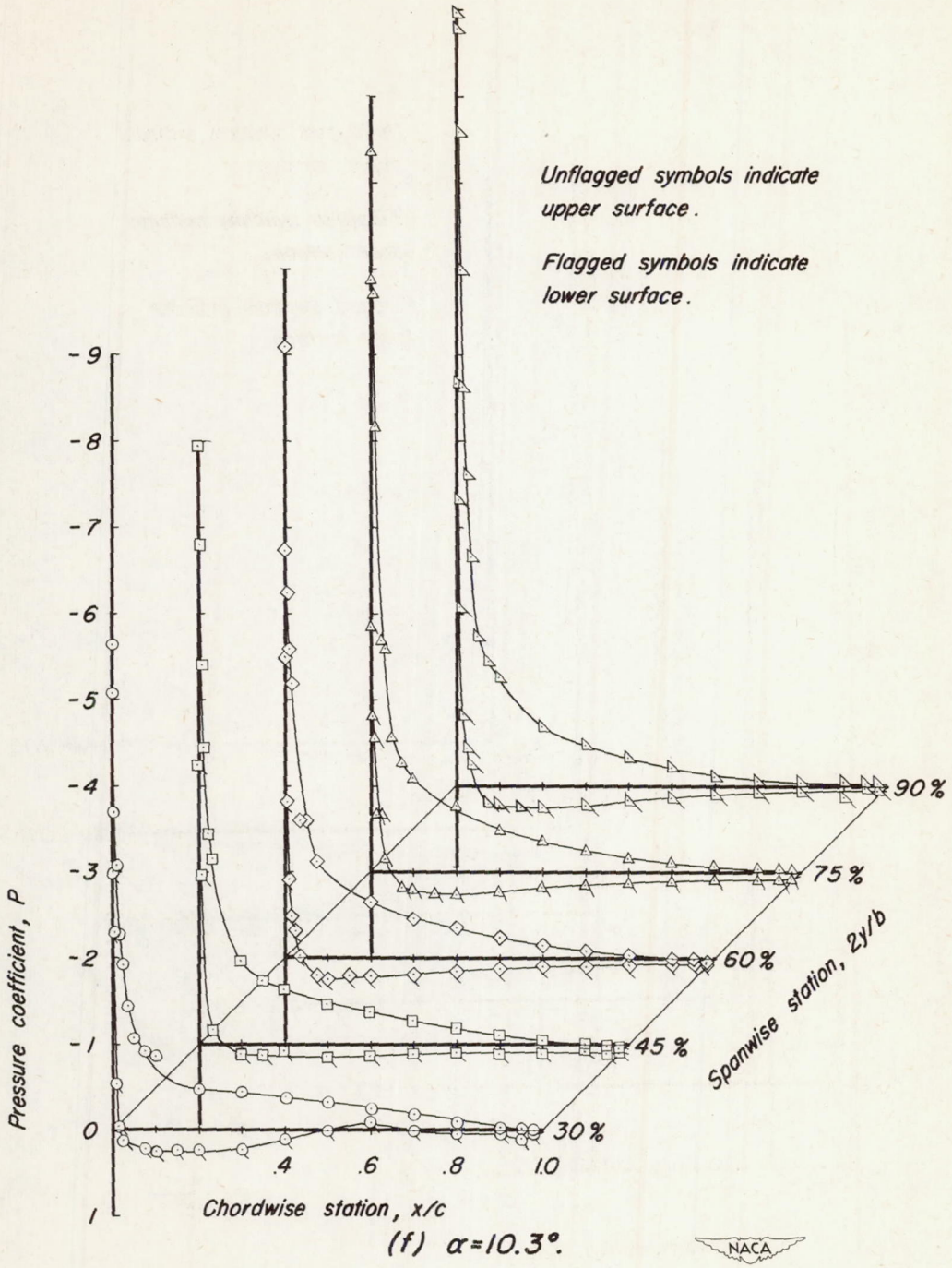

Figure 16.—Continued.

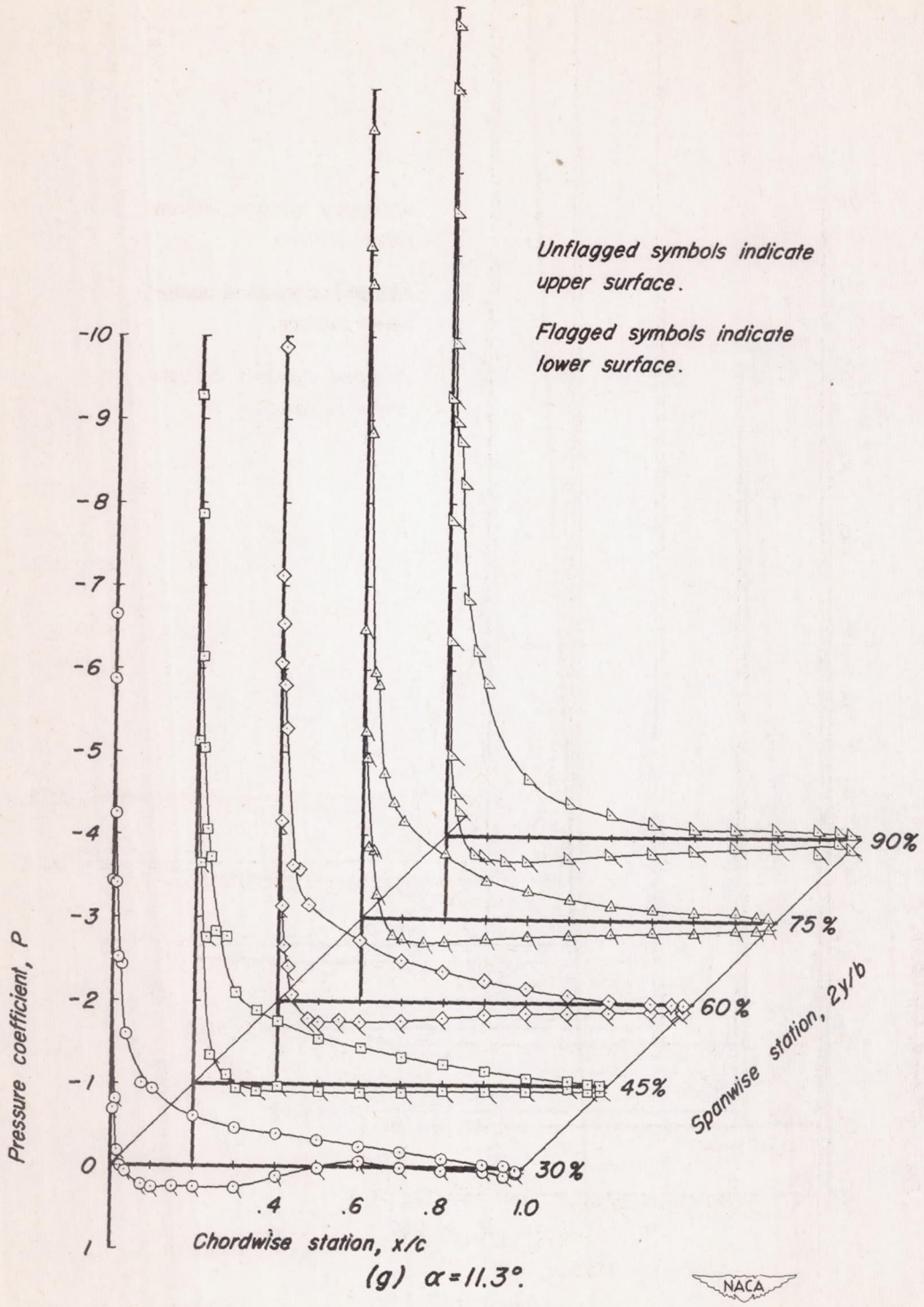

Figure 16.—Continued.

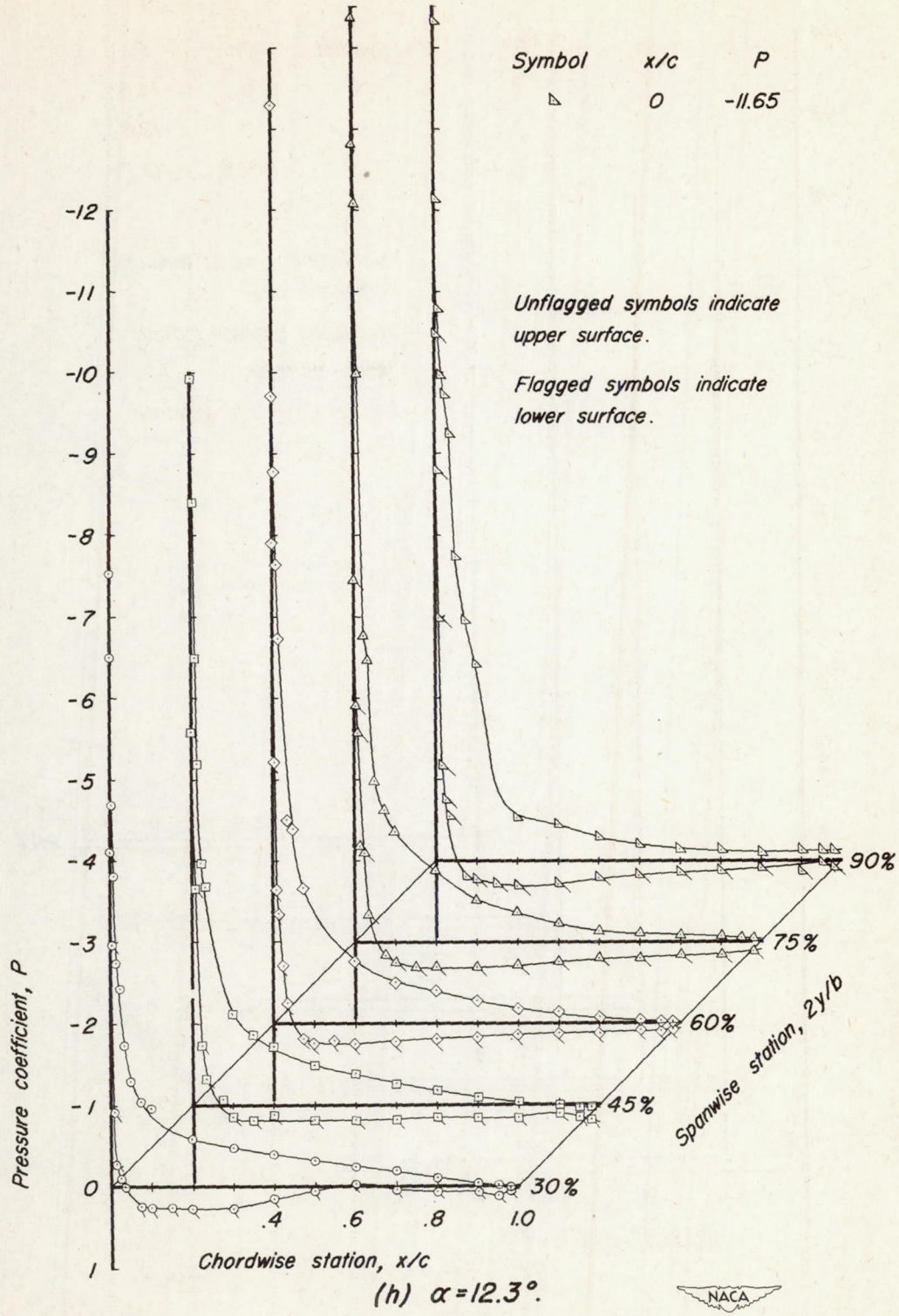

Figure 16.—Continued.

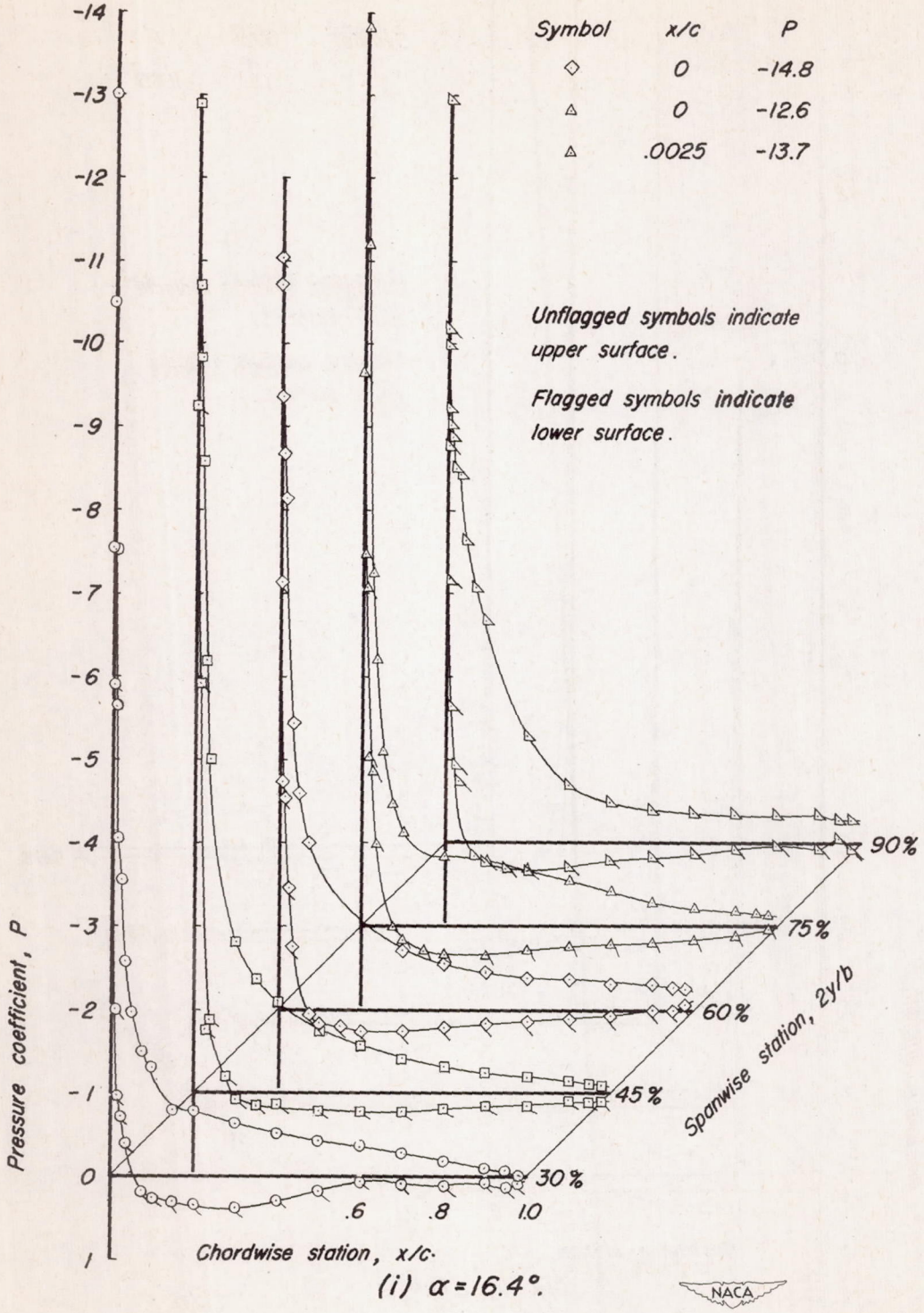

Figure 16.—Continued.

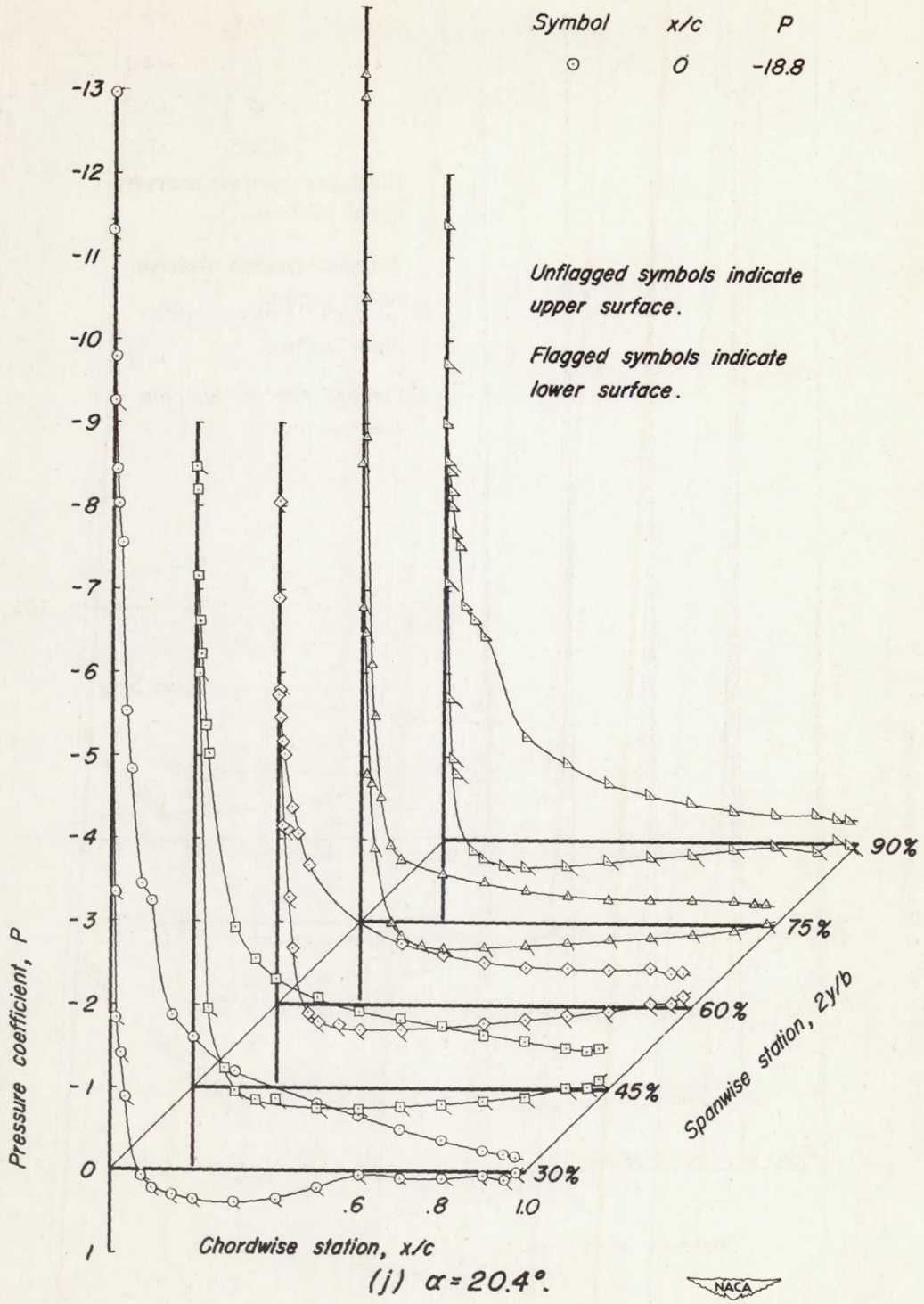

Figure 16.—Continued.

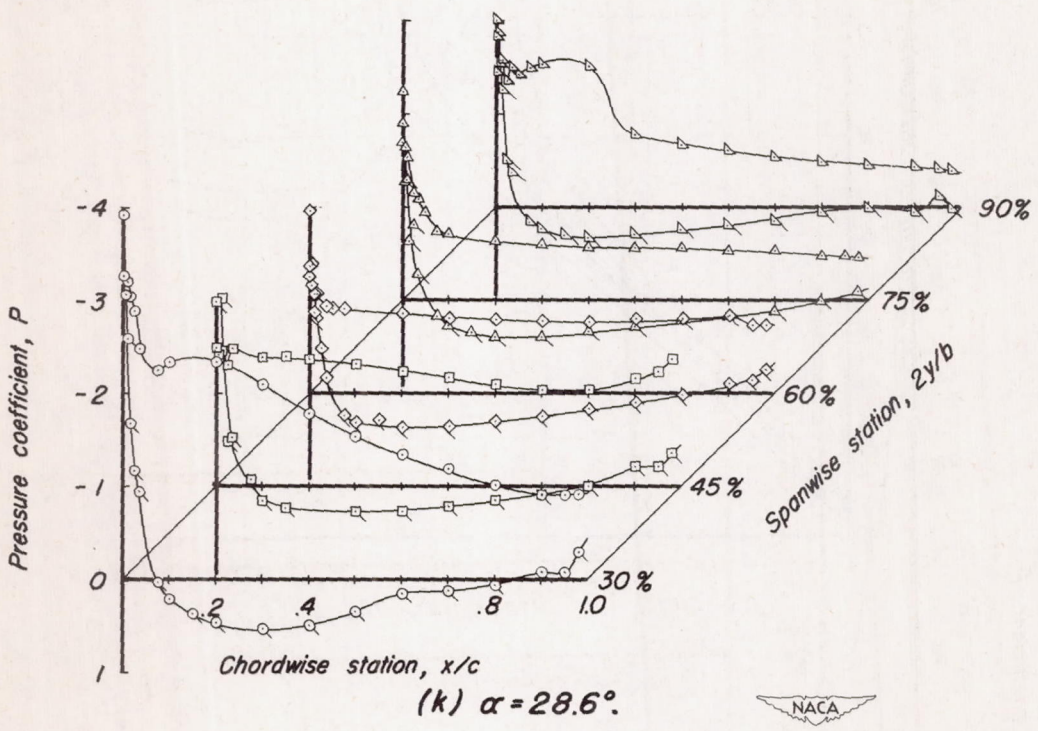

Figure 16.—Concluded.

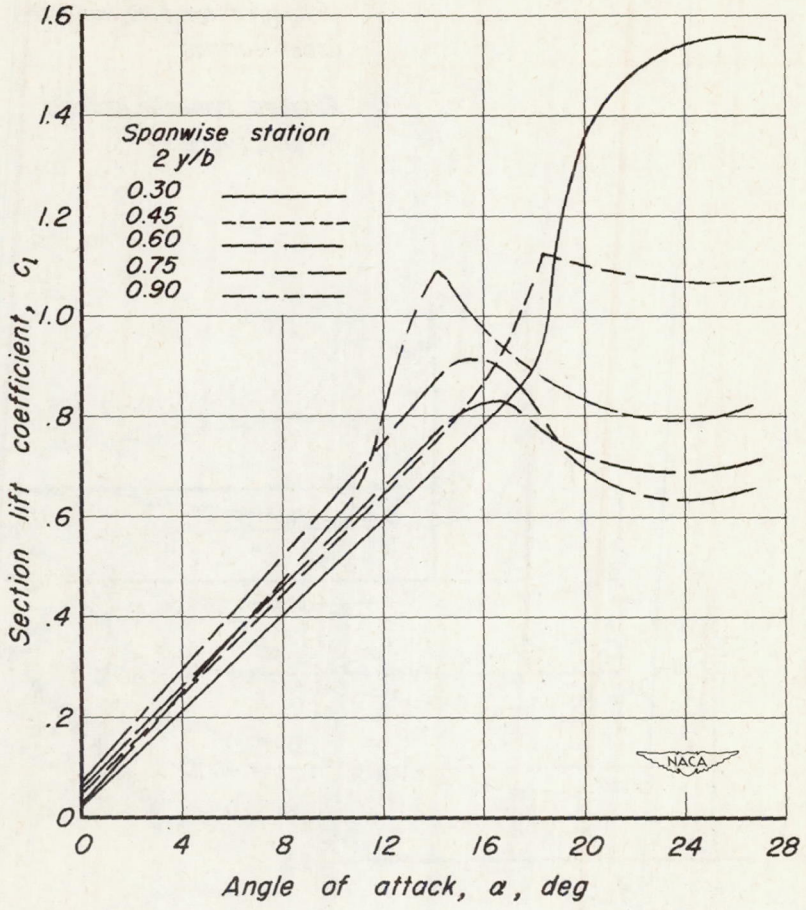

Figure 17.- Effect of area suction on the section lift curves of the 63° swept-back wing. Configuration A. C_Q=0.0029.

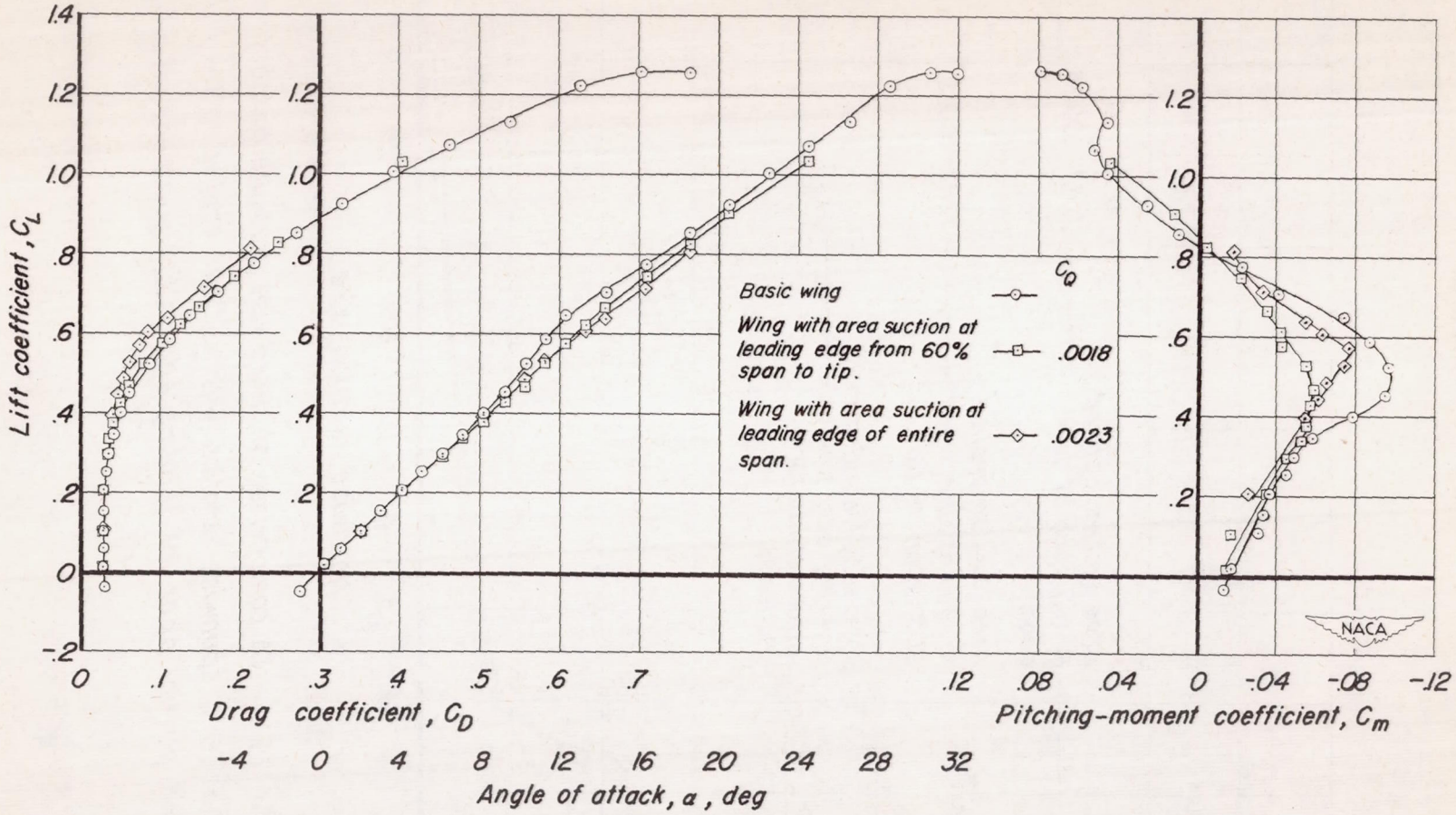

Figure 18.—A comparison of longitudinal characteristics of 63° swept-back wing with area suction applied to full span and partial span of leading edge. Configurations B and C.

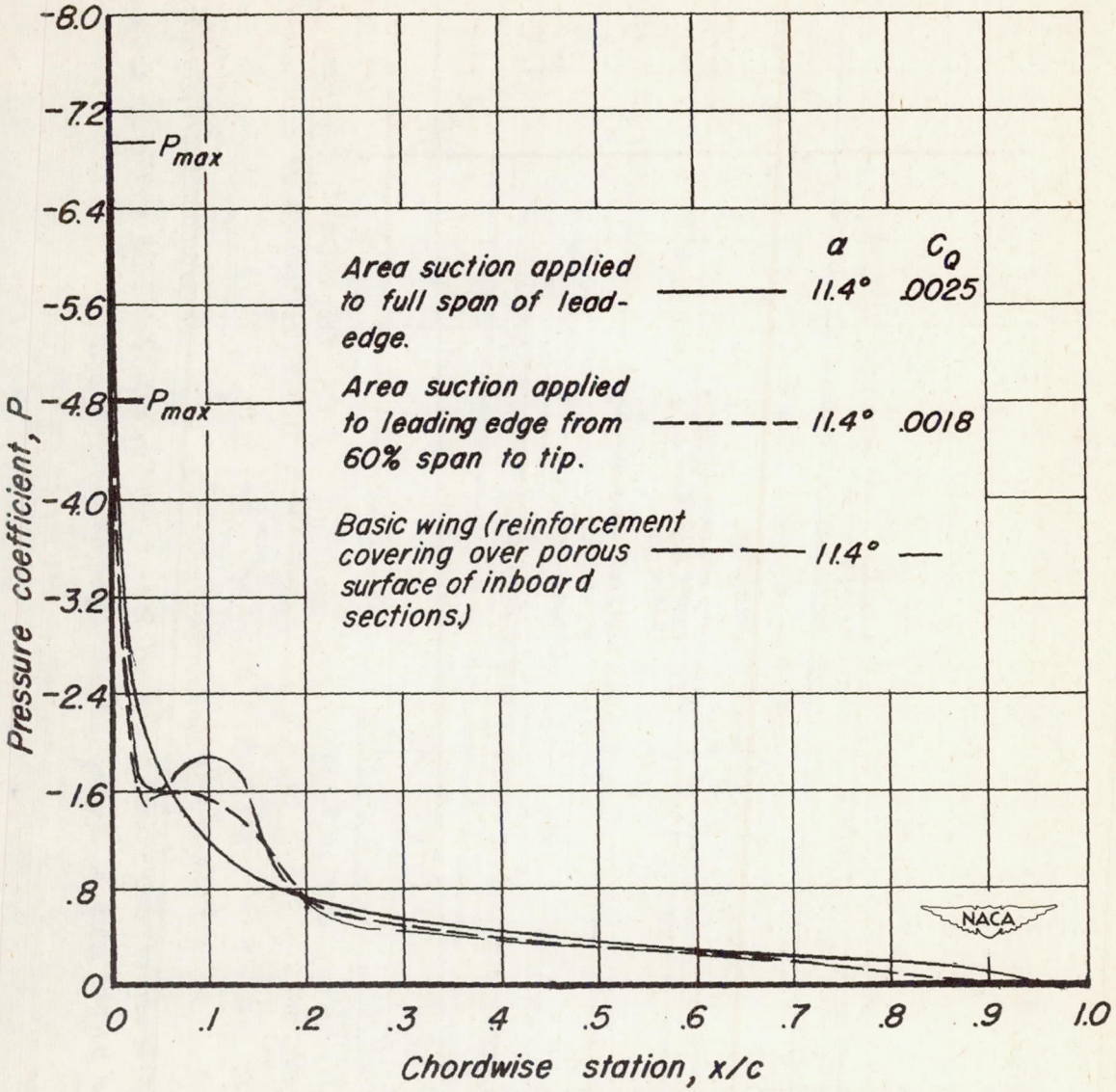

Figure 19.— A comparison of chordwise pressure distributions at the 30 % spanwise station with suction applied to the full span and partial span of leading edge. Configurations B&C.

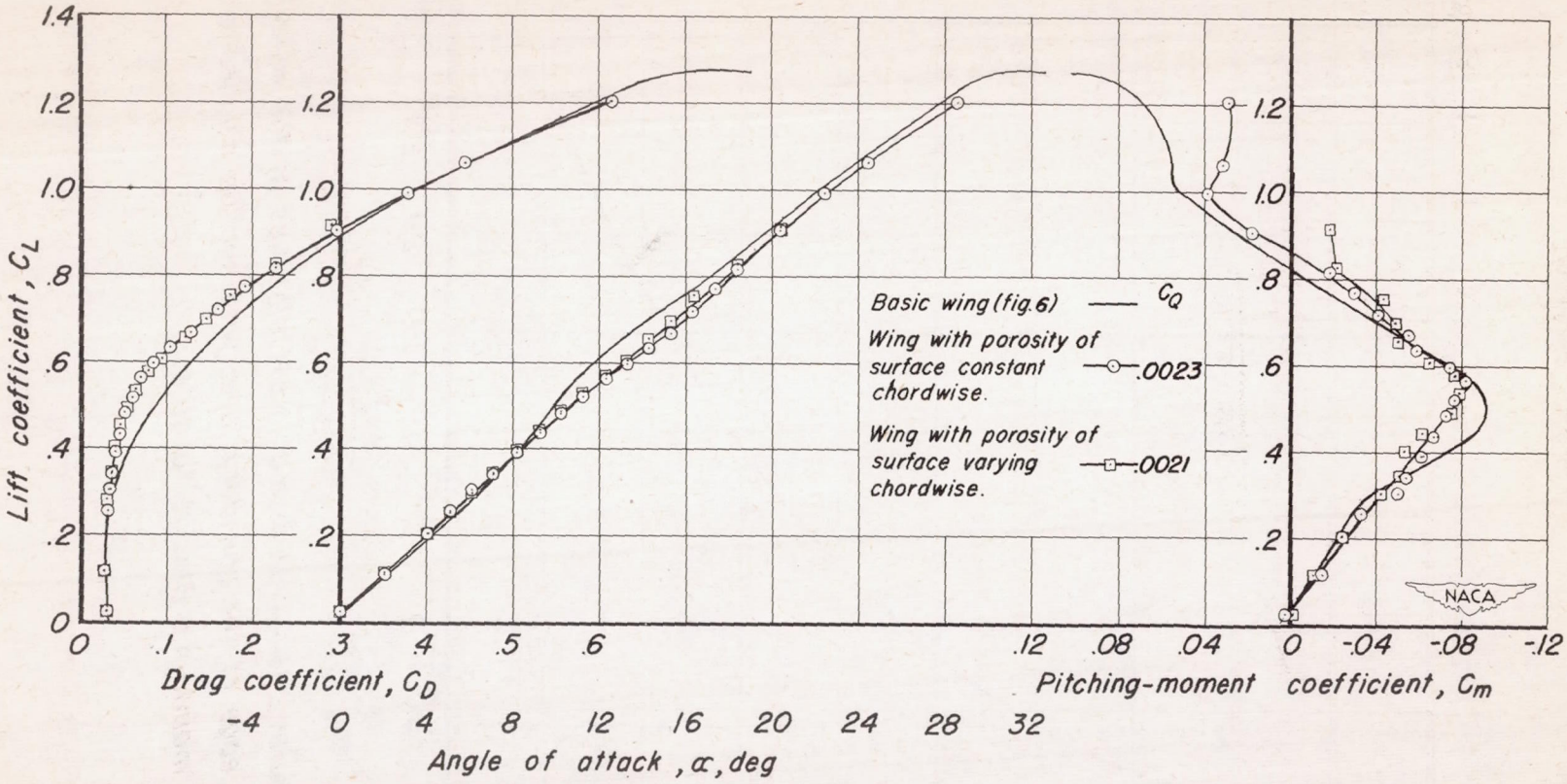

Figure 20.—Effect of varying the porosity of the surface chordwise on the longitudinal characteristics of the 63° swept-back wing with full-span application of area suction. Configurations A and F.

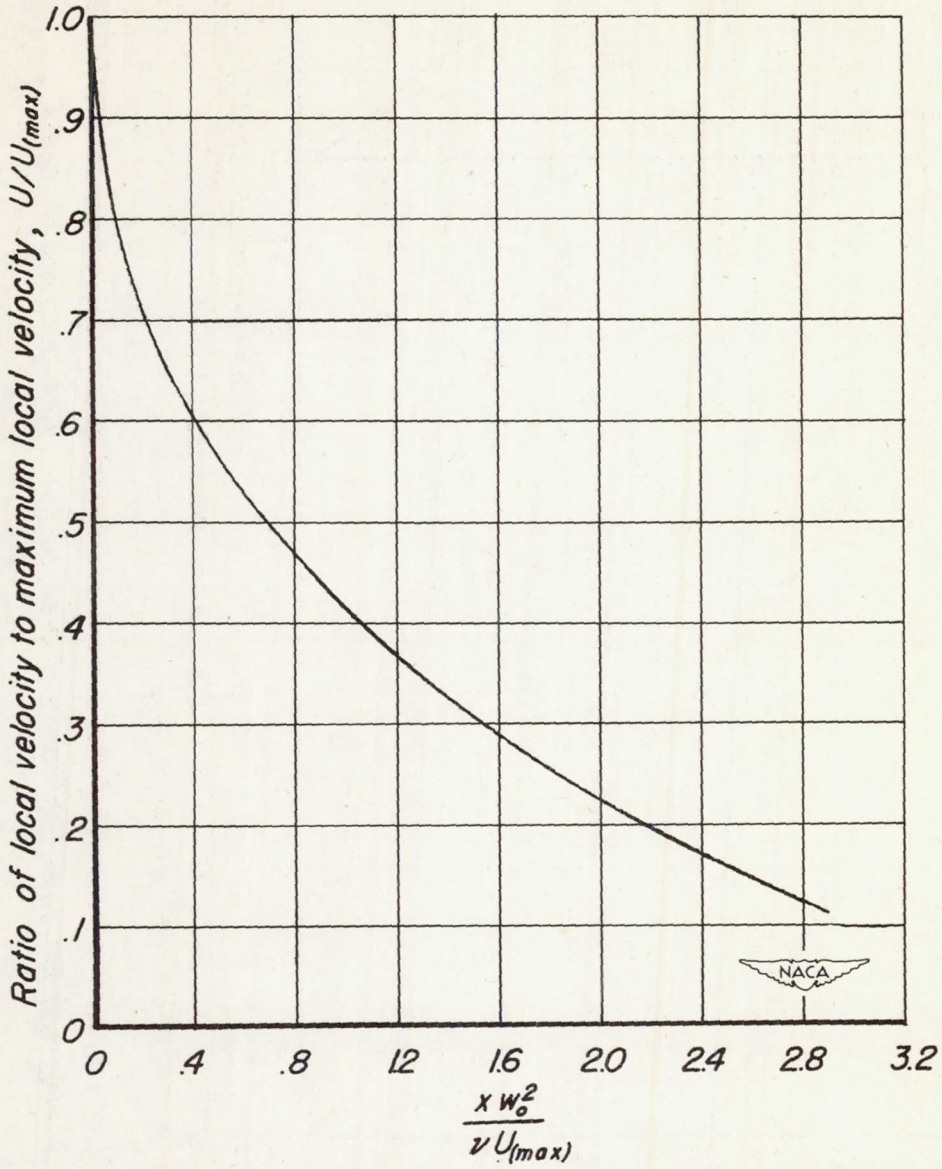

Figure 21.—Variation of local velocities at the outer edge of the boundary layer with suction applied to maintain a Blasius profile.

NACA-Langley - 11-22-50 - 430